

## TITLE PAGE

# **Upacalcet is a novel secondary hyperparathyroidism drug that targets the amino acid binding site of calcium-sensing receptor**

Hirofumi Sato, Sei Murakami, Yusuke Horii, Go Nishimura, Ryosuke Iwai, Moritaka Goto, and Naoki Takahashi

Pharmaceuticals Research Laboratories, Sanwa Kagaku Kenkyusho Co., Ltd., Mie, Japan

## **RUNNING TITLE PAGE**

**Running title** Upacalcet binds to the amino acid binding site of CaSR

Correspondence: Moritaka Goto, Pharmaceuticals Research Laboratories, Sanwa  
Kagaku Kenkyusho Co., Ltd., 363 Shiosaki, Hokusei-cho, Inabe, Mie, 511-0406.

E-mail: mo\_gotoh@skk-net.com. Tel: +81(0) 594726221

Number of text pages:43

Number of tables:1

Number of figures:9

Number of references:36

Number of words in abstract:220

Number of words in introduction:626

Number of words in discussion:1,331

### **Abbreviations**

CaSR, calcium sensing receptor; IP-1, inositol monophosphate; SHPT, secondary hyperparathyroidism; CKD, chronic kidney disease; PTH, parathyroid hormone; GPCR, G protein-coupled receptors; mGluRs, metabotropic glutamate receptors; GABA, gamma-amino butyric acid; ECD, extra cellular domain; cpm, counts per minute; dpm, disintegration per minute;

## Abstract

The human calcium-sensing receptor (CaSR) is a G-protein-coupled receptor that maintains extracellular  $\text{Ca}^{2+}$  homeostasis by regulating the secretion of parathyroid hormone. Upacicalcet is a novel positive allosteric modulator of CaSR that is used for the treatment of secondary hyperparathyroidism. In the present study, to clarify the binding site of upacicalcet to CaSR, we conducted binding studies and agonistic activity studies in HEK-293T cells expressing human CaSR (intact and mutant), and *in silico* docking-simulation analysis. As a result, upacicalcet competed with L-tryptophan and was thought to affect the amino acid binding site. In addition, the effects of substitutions at the amino acid binding site on the binding abilities to upacicalcet as well as the effects on receptor function as measured using IP-1 accumulation were examined. Upacicalcet interacted with several CaSR residues that constitute the amino acid binding site. Based on these results, we performed an *in silico* analysis and obtained a binding mode, consistent with the *in vitro* study results. Our study revealed that upacicalcet is a novel SHPT drug that targets the amino acid binding site of CaSR. Upacicalcet is expected to become a new treatment option for secondary hyperparathyroidism because the binding site differs from that of conventional drugs; consequently, it may be effective for patients who are not sensitive to conventional drugs, and it may have a superior safety profile.

## Significance statement

Upacicalcet interacts with several residues that constitute the amino acid binding site of CaSR and shows a potent positive allosteric activity. This mechanism differs from those of conventional drugs. Therefore, upacicalcet can be regarded as a “novel” SHPT drug

that acts on the amino acid binding site of CaSR.

## Introduction

Secondary hyperparathyroidism (SHPT) is a major complication in hemodialysis patients, occurring as chronic kidney disease progresses. Decreased kidney function results in an inability to activate vitamin D, resulting in inadequate calcium absorption and low calcium levels in the blood. Parathyroid hormone (PTH) secreted by the parathyroid gland plays a role in maintaining calcium and phosphorus homeostasis, but the excessive secretion of PTH in an attempt to normalize a blood calcium level that has been reduced due to reduced renal function leads to abnormal bone mineral metabolism and is associated with increased risks of fractures, ectopic calcification, and cardiac dysfunction (Cunningham et al., 2011; Go et al., 2004).

PTH secretion from the parathyroid gland is regulated by the calcium-sensing receptor (CaSR), one of the class C G protein-coupled receptors (GPCR) present on the surface of parathyroid cells. The same receptor group includes metabotropic glutamate receptors (mGluRs), GABA<sub>B</sub> receptors, taste receptors, and orphan receptors (D'Souza-Li, 2006). In the extracellular N-terminal domain of CaSR, there is a Ca<sup>2+</sup> binding pocket that senses the extracellular calcium level and a domain involved in homodimer assembly (Venus flytrap domain), and the activation of CaSR in the high calcium state suppresses the synthesis/secretion of PTH. On the other hand, under hypocalcemic conditions, the activity of CaSR is reduced, and PTH synthesis/secretion is promoted. This mechanism by which CaSR regulates PTH secretion is a key therapeutic target in SHPT (Lau et al., 2018).

Cinacalcet, evocalcet and etelcalcetide are the major calcimimetics clinically used in

SHPT treatment. All three drugs lower blood calcium levels by activating CaSR and inhibiting PTH secretion. Cinacalcet and evocalcet have been shown to interact with amino acid Glu837 in the seven-transmembrane region of CaSR, while etelcalcetide has been shown to interact with amino acid Cys482 in the extracellular region (Miyazaki et al., 2018; Alexander et al., 2015). Besides synthetic compounds, aromatic amino acids such as L-phenylalanine and L-tryptophan were also known to activate CaSR by binding to amino acid binding sites in the extracellular region (Geng et al., 2016).

Upacicalcet is a novel SHPT drug that was identified in “kokumi-flavor” studies of  $\gamma$ -glutamyl peptides, such as glutathione, and was approved in Japan for the treatment of SHPT in 2021 (Ueda et al., 1997; Broadhead et al., 2011; Amino et al., 2016; Hoy SM, 2021). Upacicalcet does not activate CaSR in the extracellular low calcium range and has a potent positive allosteric effect that enhances CaSR activity in an extracellular calcium concentration-dependent manner, similar to amino acids and cinacalcet (Miyazaki et al., 2018; Broadhead et al., 2011). On the other hand, it is not clear which part of CaSR interacts with upacicalcet, resulting in positive allosteric activity.

In this article, we conducted a study to clarify the binding sites of upacicalcet. First, we evaluated the activity of upacicalcet on CaSR as a measure of intracellular  $\text{Ca}^{2+}$  mobilization. Since upacicalcet has a positive allosteric effect similar to that of amino acid and cinacalcet, it was predicted to share a common binding site with either of these compounds. Since the chemical structure of upacicalcet is similar to that of amino acids, upacicalcet was expected to bind to the amino acid binding site of CaSR. To verify this hypothesis, we first conducted a competition study between upacicalcet and these compounds. Second, we predicted the amino acid residues of CaSR that were the most likely to interact with upacicalcet based on the previously reported crystal structure of

the ECD region of CaSR ([Geng et al., 2016](#); [Zhang et al., 2016](#)). we then performed binding studies and *in vitro* IP-1 accumulation assays for each predicted binding site using alanine-substituted mutant CaSR proteins. Finally, we performed an *in silico* docking-simulation analysis to evaluate the molecular dynamics stability and the detailed binding mode between upacalcet and human CaSR.

## Materials and Methods

Materials. Upacalcet was obtained from EA Pharma. Cinacalcet hydrochloride was obtained from Amatek Chemical. L-tryptophan was purchased from FUJIFILM Wako Pure Chemical. The synthesis of plasmid vectors encoding full-length hCaSR (both wild-type and alanine-substituted) using pBApo-CMV Pur DNA (TaKaRa Bio) as a blank vector was entrusted to TaKaRa Bio. The substitution at Cys482 resulted in replacement with tyrosine (Alexander et al., 2015). The obtained plasmids were stored at  $-20^{\circ}\text{C}$  until use. Tritium-labeled upacalcet ( $[^3\text{H}]$ -upacalcet) with a specific radioactivity of 93.1 GBq/mmol was synthesized at Sekisui Medical and stored at  $-70^{\circ}\text{C}$ .

Cell culture. HEK-293T cells (HEK) were purchased from RIKEN BRC. HEK-293T cells stably expressing hCaSR were purchased from Multispan. These cells were cultured in Dulbecco's Modified Eagle medium (DMEM; CORNING) supplemented with 10% inactivated fetal bovine serum (FBS; CORNING) and puromycin (1  $\mu\text{g}/\text{mL}$ ; Invivogen).

When the cells reached 80%–90% confluence, they were separated using trypsin and passaged; the cells were cultured at  $37^{\circ}\text{C}$  and 5%  $\text{CO}_2$ , and the number of passages was within 30 times.

Intracellular  $\text{Ca}^{2+}$  flux measurement (Calcium mobilization assay). Intracellular  $\text{Ca}^{2+}$  mobilization was measured using the Fluo-4 NW Calcium Assay Kit (Molecular Probes). CaSR-HEK cells cultured to 80%–100% confluence, the medium was removed, and 100  $\mu\text{L}$  of  $\text{Ca}^{2+}$  assay buffer (1 $\times$ HBSS, 20 mM HEPES, 2.5 mM probenecid, 1 mM

MgSO<sub>4</sub>, 0.1 mM CaCl<sub>2</sub>, 0.1% BSA) containing Fluo-4 mix dye was added. These plates were incubated at 37°C, 5% CO<sub>2</sub> for 30 min, and then incubated at room temperature for 15 min. Next, 50 µL of Ca<sup>2+</sup> assay buffer containing upacicalcet (final concentration of 0, 10, or 1000 nM) was added, and the fluorescence intensity (Ex: 485 nm, Em: 525 nm) was measured using a fluorescence plate reader (Spectramax Gemini EM; Molecular Devices) for 20 s. Then, 50 µL of Ca<sup>2+</sup> assay buffer containing various concentrations of upacicalcet and Ca<sup>2+</sup> (final concentrations, 0.1–1.5 mM) was added, and the fluorescence intensity was measured for 60 s. The RFU-fold change was calculated using the following formula, and the concentration-response curve was generated using GraphPad Prism (GraphPad Software, ver. 6.05). Each test was performed three times with triplicate measurements per concentration point.

$$\text{RFU fold change} = \frac{\text{MAX Signal level}^{*1}}{\text{MIN Signal level}^{*2}}$$

\*1: Maximum value of fluorescence intensity within 60 s.

\*2: Minimum value of fluorescence intensity within 20 s.

#### Isolation of CaSR-expressed membrane proteins from transfected HEK-293T cells.

HEK cells were cultured to 80%-90% confluence in DMEM containing 10% FBS, Opti-MEM (Invitrogen) containing 16 µg/mL of the plasmid vector encoding either the wild-type or mutant full-length *CaSR*, and 48 µL/mL of Lipofectamine 2000 (ThermoFisher). The cells were cultured at 37°C and 5% CO<sub>2</sub> for 24 hours for transfection (Trans-HEK cells). The cells were isolated by trypsin and passaged for 24 hours under the same conditions, then transferred to DMEM medium containing 1 µg/mL puromycin and passaged repeatedly until the doubling time was reached at about 20 hours. Cells were cultured to 80%-100% confluence, washed with ice-cold DPBS (Invitrogen), separated with trypsin, added to DMEM medium, and collected. The cell



clumps were obtained at  $500 \times g$  for 5 min, washed with DPBS, and centrifuged at  $1,500 \times g$  for 10 min. To the cell clumps, homogenization buffer (50 mM Tris-HCl, 1 mM  $MgCl_2$ , 10 mM KCl, pH 7.4) was added, and the cells were homogenized three times at 13,000 rpm for 30 s using a polytron homogenizer (KINEMATICA) under ice-cold conditions. The resulting cell suspension was ultracentrifuged at  $48,000 \times g$  for 20 min at  $4^\circ C$ . The homogenization and ultracentrifugation were repeated three times, and the protein concentration of the obtained membrane protein fraction solution was assayed using the BCA protein assay kit (Pierce), diluted to 2 mg/mL, and stored at  $-80^\circ C$  until use. The cell membranes of HEK cells and CaSR-HEK cells were prepared using the same procedure.

Confirmation of CaSR expression using western blot analysis. HEK cells, HEK-CaSR cells and Trans-HEK cells with a doubling time of about 20 hours were collected, washed in DPBS, and RIPA buffer A (BioDynamics Laboratory) containing protease inhibitors was added to lyse the cells. The lysis solution was centrifuged at 15,000 rpm at  $4^\circ C$  for 20 min, and the protein concentration in the supernatant was measured using the BCA protein assay kit. Laemmli buffer (Bio Rad) containing 2-mercaptoethanol (One-tenth of the amount of laemmli buffer) and Tris-HCl (Moderate amount; for protein concentration adjustment) were added to make the protein concentration 2 mg/mL, and the solution was heated at  $95^\circ C$  for 5 min. Mini PROTEAN TGX gel 4%–20% (Bio-Rad) was set in the electrophoresis device (Mini PROTEAN Tetra cell, Bio-Rad) filled with  $1\times$  Tris/Glycine/SDS Buffer, and after sample application, the device was run at 200 V. The gels were transferred to PVDF membranes using Trans-Blot Turbo Mini PVDF Transfer Packs (Bio-Rad) at 25 V for 30 min. The

transferred membrane was blocked with PVDF blocking reagent (TOYOBO). Anti-CaSR antibody [5C10, ADD] (ab19347; abcam) was used as the primary antibody for CaSR detection. Primary antibody was diluted 2000-fold with Can Get Signal solution 1 (TOYOBO). Anti-mouse IgG H&L HRP (ab205719; Bio-Rad) was used as the secondary antibody. Secondary antibody was diluted 5000-fold with Can Get Signal solution 2 (TOYOBO). Transfer membranes treated with the primary and secondary antibodies were colorized using the ECL prime Western Blotting Detection System (Amersham) and photographed using ChemiDoc XRS Plus (Bio-Rad).

Competitive binding study of tryptophan and cinacalcet using a scintillation proximity assay. WGA PEI Type A PVT SPA Scintillation Beads (PerkinElmer) were suspended in binding assay buffer (50 mM Tris-HCl, 1 mM MgCl<sub>2</sub>, 0.5% CHAPS, pH 7.4), and HEK or HEK-CaSR membrane protein solution was added and preincubated at 4°C for 2 hours. Binding assay buffer or cold upacalcet containing binding assay buffer (final concentration, 100 μM) was added to the beads/membrane protein solution. In addition, cold upacalcet containing binding assay buffer (final concentration,  $1.0 \times 10^{-11}$ – $10^{-4}$  M), L-tryptophan containing binding assay buffer (final concentration, 0.03–30 mM) or cinacalcet HCl containing binding assay buffer (final concentration,  $1.0 \times 10^{-11}$ – $10^{-4}$  M) was added, and 15,000 dpm of [<sup>3</sup>H]-upacalcet was added and allowed to react for 60 min at room temperature. MicroBeta2 (Perkin Elmer) was used to count the measured values, and the specific binding was calculated from the obtained values using the following formula. The IC<sub>50</sub> values of upacalcet and L-tryptophan were calculated using GraphPad Prism (GraphPad Software, ver. 6.05) based on the obtained values. Each test was performed three times with triplicate measurements per concentration

point.

$$\text{Specific Binding (cpm)} = \text{Total Binding}^{*3} - \text{Non-specific Binding}^{*4}$$

\*3: Counts in the absence of cold upacicalcet (cpm)

\*4: Counts in the presence of cold upacicalcet (cpm)

Evaluation of upacicalcet relative binding abilities to wild-type and various mutant CaSR proteins using a scintillation proximity assay. WGA PEI Type A PVT SPA Scintillation Beads were suspended in binding assay buffer, and various Trans-HEK membrane protein suspensions were added and preincubated at 4°C for 2 hours. Binding assay buffer or cold upacicalcet containing binding assay buffer (final concentration, 100 µM) was added to the beads/membrane protein solution. Next, 40,000 dpm of [<sup>3</sup>H]-upacicalcet was added and allowed to react for 60 min at room temperature. MicroBeta2 (Perkin Elmer) was used to count the measured values, and the specific binding was calculated from the obtained values using the same formula as described above. The relative binding ability of each mutant CaSR protein was calculated using the following formula when the specific binding of upacicalcet to wild-type CaSR obtained in the all test was set at 100%. Each test was performed three times with triplicate measurements per concentration point.

$$\text{Relative binding (\%)} = \frac{\text{Specific Binding of mutant CaSR (cpm)}}{\text{Specific Binding of WT CaSR (cpm)}} \times 100$$

Statistical differences in the relative binding of upacicalcet to each mutant CaSR vs. wild-type CaSR were determined by a one-way ANOVA followed by the Dunnett's multiple comparison, and *P* values <0.05 were to be considered statistically significant.

Molecular Docking Study. Molecular docking was performed using the Schrödinger package program (Schrödinger LLC, New York, US). A three-dimensional model of upacalcet was generated using the LigPrep program in the Schrödinger suite. The ligands were minimized by the OPLS3e force field (Roos et al., 2019). The CaSR ECD crystal structures (PDB 5K5S, 5FBH and 5FBK; all three crystal structures were reported by the other research groups previously, Geng et al., 2016; Zhang et al., 2016) were prepared using the Protein Preparation Wizard program in the Schrödinger suite (Sastry et al., 2013). All water molecules were deleted. In addition,  $\text{Ca}^{2+}$  at calcium binding site 2 was modified to  $\text{Cl}^-$  in PDB 5K5S and  $\text{Ca}^{2+}$  at the calcium binding site 3 in both PDB 5K5S and 5FBK were deleted (Geng et al., 2016; Zhang et al., 2016). Induced fit docking was performed using the automated extended sampling protocol in the Schrödinger suite (Sherman et al., 2006). This first performs several initial dockings with the side chains either removed and with the van der Waals potential softened according to their flexibility. The side chains are then rebuilt, and those within 5 Å of the ligand are optimized using Prime program in the Schrödinger suite. The ligand was redocked into the new receptor structure using the Glide SP algorithm in the Schrödinger suite (Friensner et al., 2004) and a standard potential. The receptor grid was centered on the L-tryptophan (PDB 5K5S) or the cyclomethyltryptophan (PDB 5FBH, 5FBK) and was generated using the OPLS3e force field (Roos et al., 2019). Upacalcet was docked to chain A and B of PDB 5K5S, 5FBH and 5FBK using the extended sampling protocol and the following core constraints: the alpha-amino group, carboxyl group, alpha-carbon, and beta-carbon of the ligand in the co-crystal structure had to overlap with the root mean square deviation (RMSD) within 1 Å.

Ligand-protein interaction analysis of docking poses. To derive the interaction fingerprints of all docking poses, we used Maestro's "Interaction Fingerprint Panel" in the Schrödinger suite (Deng et al., 2004; Singh et al., 2006). This method uses bits to describe the presence of different kinds of chemical interactions between the ligand and the binding site residues of the target receptor. For this purpose, a distance cutoff value is defined for the binding site, and residues containing atoms within the specified cutoff distance from the ligand atom are included in the interaction set. In this study, we used only the interaction fingerprints of the sidechain interaction because we were interested in changes in relative binding abilities resulting from amino acid substitutions in CaSR. To select amino acids in CaSR with the potential to interact with upacalcet, the interaction fingerprints of the sidechain interaction were used for the output docking poses to determine the frequency of the interacting amino acids. We also used the interaction fingerprints of the sidechain interaction to filter out docking poses that were consistent with the relative binding abilities to mutant CaSR proteins.

Inositol phosphate measurement (IP-1 assay). The intracellular accumulation of inositol monophosphate was measured using the Homogenous Time Resolution Fluorescence (HTRF) IP-one Tb kit (Cisbio). This assay quantifies the accumulation of inositol 1-monophosphate (IP-1), a degradation product of inositol 1,4,5-trisphosphate (IP-3), and is stable in the presence of LiCl (Zhang et al., 2010). HEK cells were transiently transfected with plasmids encoding wild-type or mutant full-length *CaSR* using the same procedure as that used to prepare the membrane proteins. After overnight incubation at 37°C and 5% CO<sub>2</sub>, the medium was removed and each concentration of Ca<sup>2+</sup> and presence or absence of 100 μM upacalcet solutions of each concentration

dissolved in assay buffer (1×HBSS, 20 mM HEPES, 1 mM MgSO<sub>4</sub>, 50 mM LiCl, 0.1% BSA) were added and incubated at 37°C and 5% CO<sub>2</sub> for 2 hours. After that, IP1-d2 conjugate and Anti-IP1 cryptate were added, mixed well, and the fluorescence intensity (fluorescence wavelength; 665/620 nm) was measured using a luminescence fluorescence plate reader (POWERSCAN4, DS pharma). From the obtained fluorescence intensity, the ratio at each concentration point was calculated according to the following formula.

$$\text{Ratio} = \frac{\text{Fluorescence 665 nm}}{\text{Fluorescence 620 nm}} \times 10000$$

The IP-1 concentration (nmol/L) at each concentration point was calculated using the 4-parameter calibration curve by GraphPad Prism (GraphPad Software, ver. 6.05) based on the ratios of the standard CaSR measured simultaneously. The IP-1 ratio (%) of each mutant CaSR was calculated based on the wild-type IP-1 concentration of E<sub>max</sub> as 100%. Each test was performed in duplicate at each concentration point, and the measurements were repeated three times except in the case which the concentration-dependent IP-1 accumulation disappeared by the mutation.

Molecular dynamics simulations. Molecular dynamics simulations of the selected docking poses were performed using the Desmond program in the Schrödinger suite (Bowers et al., 2006). Each protein-ligand complex was placed in a cubic box with a buffer distance of 10 Å to create a hydration model and ionized to a concentration of 0.15 M NaCl. The overall charge of each system was neutralized by the addition of Na<sup>+</sup> or Cl<sup>-</sup> ions, as appropriate.

The OPLS3e all-atom force field ([Roos et al., 2019](#)) was used to describe all molecules. For water, the simple point charge (SPC) model ([Jorgensen et al., 1983](#)) was used to model hydration. For system minimization and relaxation, the NPT ensemble was used. Each simulation was run for a total of 120 ns, and the simulations were repeated three times for each system. Temperature and pressure were kept constant at 300 K and 1.01325 bar, respectively, throughout the simulation. The data analyses, such as RMSD and the ligand interaction fingerprints, were performed using the simulation interaction diagram program in the Schrödinger suite.

## Results

### Upacicalcet is a positive allosteric modulator for CaSR

Upacicalcet is an amino acid-derived compound that was discovered during the study of the “kokumi-flavor” of  $\gamma$ -glutamyl peptides, such as glutathione (Ueda et al., 1997). While glutathione analogs have a linear skeleton, upacicalcet has an aromatic ring, and its structure is similar to that of aromatic amino acids such as L-tryptophan (Fig. 1A). In addition, amino acids and glutathione analogs are known to have positive allosteric effects on CaSR, and similar positive allosteric effects have been also reported for cinacalcet (Broadhead et al., 2011; Amino et al., 2016; Conigrave et al., 2002; Conigrave et al., 2004; Conigrave et al., 2006b; Nemeth et al., 2004). First, to characterize the agonistic activity of upacicalcet for CaSR, we evaluated the effect of hCaSR on extracellular  $\text{Ca}^{2+}$  concentration-dependent intracellular  $\text{Ca}^{2+}$  mobilization in the presence of upacicalcet in HEK-293 cells. At an extracellular  $\text{Ca}^{2+}$  concentration of 0.1 mM, upacicalcet did not affect intracellular  $\text{Ca}^{2+}$  mobilization up to 1,000 nM; at concentrations of 0.4 mM of extracellular  $\text{Ca}^{2+}$  or higher, however, upacicalcet increased intracellular  $\text{Ca}^{2+}$  mobilization in a concentration-dependent manner (Fig. 2). On the other hand, the maximum effect of intracellular  $\text{Ca}^{2+}$  mobilization was unchanged with or without upacicalcet treatment. These data indicate that while upacicalcet does not activate CaSR in the low extracellular  $\text{Ca}^{2+}$  concentration range (less than 0.1 mM), it does enhance  $\text{Ca}^{2+}$  action in the high  $\text{Ca}^{2+}$  concentration range. Thus, upacicalcet is a pure positive allosteric modulator that enhances CaSR signaling in an extracellular  $\text{Ca}^{2+}$  concentration-dependent manner, without exerting agonist effects on CaSR.



### **Upacicalcet and tryptophan bind to the same binding site of CaSR**

Since upacicalcet is a positive allosteric modulator of CaSR similar to amino acids and the chemical structure of upacicalcet is similar to that of aromatic amino acids, we hypothesized that the binding site of upacicalcet is the same as that for amino acids. To confirm this hypothesis, the effect of L-tryptophan on the binding ability of upacicalcet to CaSR was evaluated using a scintillation proximity assay. First, to confirm the binding of upacicalcet to CaSR, we performed a competition study between cold and [<sup>3</sup>H]-upacicalcet using HEK-CaSR and HEK membrane proteins. The results showed specific binding only to the HEK-CaSR membrane protein, and the binding was inhibited in a concentration-dependent manner by cold upacicalcet (IC<sub>50</sub>: 8.2 nM; Fig. 3A, Table S1). Additionally, the specific binding of upacicalcet with hCaSR was reduced with the addition of L-tryptophan in a concentration-dependent manner (IC<sub>50</sub>: 4.3 mM; Fig. 3B, Table S1). On the other hand, cinacalcet did not affect the binding of upacicalcet to hCaSR at concentrations of up to 100 μM (Fig. 3C).

### **Prediction of residues thought to be important for upacicalcet binding based on the crystal structure of the CaSR ECD region**

The specific binding of upacicalcet to CaSR was inhibited by L-tryptophan in a concentration-dependent manner, strongly suggesting that upacicalcet acts on the amino acid binding site in the extracellular region of CaSR. Therefore, we elucidated the detailed binding mode of upacicalcet to CaSR. We evaluated the effect of alanine substitutions at amino acid residues of CaSR that were thought to be important for upacicalcet binding on the actual relative binding abilities of [<sup>3</sup>H]-upacicalcet to mutant CaSR-HEK membrane fractions.

To select the mutation site of CaSR, docking studies comparing upacalcet and the previously reported crystal structure of the ECD region of CaSR ([Geng et al., 2016](#); [Zhang et al., 2016](#)) were performed. As a result, a total of 276 docking poses were output. The breakdown was 49 and 47 poses for PDB 5K5S chain A and chain B; 40 and 49 poses for PDB 5FBH chain A and chain B; 42 and 49 poses for PDB 5FBK chain A and chain B, respectively (Fig. 4). Then, to determine the amino acid side chains that may interact with upacalcet, the frequency of interaction of each amino acid was confirmed by calculating the interaction fingerprints of the sidechain interaction for all docking poses (Table 1). The amino acids that frequently interacted with upacalcet or that are known to interact with L-tryptophan and cyclomethyltryptophan were selected as candidate substitution sites ([Geng et al., 2016](#); [Zhang et al., 2016](#)) except for Tyr218 and Asn64, which were considered to have low priorities based on the binding mode of L-tryptophan, the structure of the residues, and the distance between the molecules. As a result of this analysis, eight amino acids (Arg66, Trp70, Ser147, Ser170, Ser272, Glu297, Ser302, and Ile416) were selected as the sites of alanine substitution in CaSR (Fig. 4, Fig. 5). In addition, Cys482, the binding site of etelcalcetide ([Alexander et al., 2015](#)), and Glu837, that of cinacalcet ([Leach et al., 2016](#)), were selected as mutation targets for the evaluation of mutated CaSR proteins.

### **Several of the amino acid residues that form the amino acid binding site of CaSR are important for the binding of upacalcet**

Plasmid vectors encoding various full-length CaSR proteins were introduced into HEK-293 cells to express the various mutated CaSR proteins. The expressions of the various CaSR proteins were evaluated using western blotting. First, the specificity of

the antibody was confirmed by evaluating the whole proteins of HEK-CaSR, HEK and HEK-WT expressing wild-type CaSR (Fig. S1). Then, the amounts of expressed various mutant CaSR proteins were evaluated, and there was no difference in expression levels (Fig. 6A). Subsequently, we examined the effect of substitutions (C482Y, etelcalcetide binding residue; E837A, cinacalcet binding residue) in CaSR on the binding ability of upacicalcet. The relative binding of [<sup>3</sup>H]-upacicalcet to the mutated CaSR proteins did not decrease for either substitution when the wild-type binding ability was 100% (Fig. 6B).

We then evaluated the effects of alanine substitutions at residues Ser147 and Ser170 in the extracellular region of CaSR, as these residues are known to be important for the binding of amino acids to CaSR (Geng et al., 2016; Zhang et al., 2002; Silve et al., 2005). As a result, the relative binding abilities of [<sup>3</sup>H]-upacicalcet to both mutated CaSR proteins were greatly decreased to  $\leq 20\%$  of that seen for wild-type CaSR (Fig. 6B). It is believed that hydrogen bonds are formed between the serine side chains (hydroxyl groups) of Ser147 and Ser170 of CaSR and the hydroxyl and carboxyl groups of ligand amino acids ( $\alpha$ -amino acids *in vivo*, especially aromatic amino acids). The replacement of serine with alanine is thought to have reduced the ability to form hydrogen bonds with the hydroxyl and carboxyl groups of upacicalcet. This result is supported by the fact that the CaSR-activating activity of a metabolite with the amino group removed from upacicalcet was evaluated using intracellular Ca<sup>2+</sup> mobilization, but the activity was lost (data not shown).

Next, we evaluated the effects of alanine substitutions at Trp70, Glu297 and Ile416 of CaSR, since these residues reportedly interact with L-tryptophan (Geng et al., 2016). As a result, the relative binding abilities to W70A and E297A were significantly

decreased to  $\leq 20\%$  of that seen for wild-type CaSR; these results were comparable to those for S147A and S170A. As well, the relative binding to I416A also showed a significant decrease to about 30% of that for the wild-type CaSR (Fig. 6B).

Finally, we evaluated the effects of alanine substitutions at three amino acid residues, Arg66, Ser272, and Ser302; these residues were selected as a result of previously reported induced fit-docking between the crystal structure of the ECD region of CaSR (Geng et al., 2016; Zhang et al., 2016) and upacalcet, as shown in Table 1. R66A showed a significant decrease ( $P < 0.001$ ) in upacalcet binding ability to about 30% of that for wild-type CaSR. S302A also showed a significant ( $P < 0.05$ ) decrease in binding ability, however, the effect was quite weak compare to that of other residues (approximately less than 40% reduction vs. wild-type CaSR). Furthermore, no decrease in upacalcet binding ability was observed for S272A (Fig. 6B). When the structure of upacalcet was compared with those of aromatic amino acids, such as L-tryptophan and phenylalanine, these residues were thought to interact with methyl, chloro and sulfo groups, which are characteristic of upacalcet only, and Arg66 was especially important.

### **IP-1 assay results for each mutant CaSR protein support the binding ability results**

The above results suggested that upacalcet binds to the amino acid binding site of CaSR and that the CaSR residues that are important for this binding are as follows: (1) residues that interact with amino acid alpha-amino and carboxyl groups (Ser147, Ser170), (2) residues that commonly interact with aromatic amino acids such as L-tryptophan (Trp70, Glu297, Ile416), and (3) residues that interact only with upacalcet (Arg66). We attempted to improve the confidence of the relative binding

ability results by evaluating the functional aspects of the receptor as well. We transfected HEK-293 cells with plasmid vectors encoding wild-type or mutant forms of *CaSR*, as in the relative binding ability evaluation, and generated HEK-293 cells transiently expressing these mutated *CaSR* proteins. The effect of each mutation on calcium signaling and the effect of upacalcet (100  $\mu$ M) on calcium signaling were evaluated using the intracellular accumulation of IP-1 as an indicator. Intracellular calcium release is frequently triggered by non-G-protein mechanisms such as  $\text{Ca}^{2+}$ -permeable channels, calcium pumps, and calcium transporters, so optimization of the evaluation system is necessary to measure  $\text{Ca}^{2+}$  responsiveness. The IP-1 assay measures IP-1 rather than the short-lived IP-3 generated by the phospholipase C (PLC) pathway via GPCR Gq signaling, in which the IP-3–IP-2–IP-1–inositol dephosphorylation pathway is stopped by the addition of lithium chloride and accumulates in IP-1. IP-1 assay is often used to measure the activity of GPCRs including *CaSR* (Zhang et al., 2010; Walter et al., 2013; Geng et al., 2016). In addition, the concentration of upacalcet added (100  $\mu$ M) was selected under conditions at which the wild type was fully saturated in the pre-test of the IP-1 assay for the purpose of confirming the maximum effect of the wild type and the mutant.

First, we confirmed the effect of  $\text{Ca}^{2+}$  and upacalcet in HEK-293T cells transiently expressing wild-type *CaSR*. As a result, we observed an extracellular  $\text{Ca}^{2+}$  concentration-dependent accumulation of IP-1 and a shift in the sigmoid function toward a lower concentration in the presence of upacalcet (Fig. 7A). In this manner, we confirmed the validity of the assay method and the positive allosteric effect of upacalcet. We then evaluated the effects of substitutions (C482Y, E837A) at the *CaSR* site where upacalcet binds. Similar to previous reports (Alexander et al., 2015;

Jacobsen et al., 2017), no change for C482Y and E837A were observed (Fig. S2A). In the presence of upacalcet, the  $E_{\max}$  was slightly decreased for E837A, compared with the wild type, but no change was observed for C482Y (Fig. 7B).

Next, we evaluated S147A, S170A, and E297A, which have been reported as protein mutations that significantly reduce the  $\text{Ca}^{2+}$  response (Geng et al., 2016; Zhang et al., 2002; Silve et al., 2005) (Fig. S2B). Surprisingly, S147A, S170A, and E297A conferred a marked recovery effect on  $\text{Ca}^{2+}$  responsiveness in the presence of upacalcet (Fig. 7C). Reportedly, the change in  $\text{Ca}^{2+}$  response conferred by W70A is also greatly decreased, similar to the above results observed for S147A, S170A, and E297A (Ling et al., 2021). We also observed a significant decrease in the  $\text{Ca}^{2+}$  response in the presence of W70A (Fig. S2C). However, the recovery of  $\text{Ca}^{2+}$  responsiveness in the presence of W70A and upacalcet was less marked, unlike the results seen for S147A, S170A, and E297A (Fig. 7D). Although previous findings regarding  $\text{Ca}^{2+}$  responsiveness in the presence of I416A and upacalcet are not available, no changes were observed in our study (Fig. S2C). On the other hand,  $\text{Ca}^{2+}$  responsiveness in the presence of upacalcet was decreased (Fig. 7D). Furthermore,  $\text{Ca}^{2+}$  responses to the R66A, S272A, and S302A substitutions were unchanged or showed a slight decrease (Fig. S2D). The substitution of Arg66 with histidine has been reported to decrease the  $\text{Ca}^{2+}$  response (Geng et al., 2016).  $\text{Ca}^{2+}$  responsiveness in the presence of upacalcet was decreased for R66A, slightly decreased for S302A, and unchanged for S272A, compared with the wild type (Fig. 7E).

The results of the IP-1 assay in the presence of upacalcet paralleled the relative binding results closely. In particular, mutations resulting in a large decrease in relative binding ability also caused a large decrease in  $\text{Ca}^{2+}$  responsiveness in the presence of

upacalcet in the IP-1 assay. However, mutations targeting three residues (Ser147, Ser170, and Glu297), which are considered important for amino acid binding, resulted in a strong  $\text{Ca}^{2+}$  response recovery. Although aromatic amino acids have been shown to have a weak effect on  $\text{Ca}^{2+}$  response recovery in previous reports (Zhang et al., 2002; Silve et al., 2005), the effect of upacalcet was much more potent than that of aromatic amino acids. As an additional test, we evaluated the effect of amino acids on the recovery of  $\text{Ca}^{2+}$  responsiveness to mutant CaSR protein (S170A), the  $\text{Ca}^{2+}$  response for which was greatly reduced in the IP-1 assay. As a result, in the presence of 50 mM of L-tryptophan, there was a slight recovery of the  $\text{Ca}^{2+}$  response in the high concentration range of extracellular  $\text{Ca}^{2+}$ . On the other hand, no recovery was observed in the presence of 50 mM of glycine (data not shown).

### **Binding mode of upacalcet to CaSR**

Based on the results of the above studies and using molecular dynamics simulations, we found a binding mode that is consistent with the experimental results. In brief, we considered interacting residues (Arg66, Trp70, Ser147, Ser170, Glu297 and Ile416) that clearly showed reduced binding ability and activity in the IP-1 assay compared to WT. In addition, we considered that Ser302, which showed a slight decrease in binding ability, and Ser272, which showed no decrease, did not contribute as much to the binding of upacalcet to CaSR compared to other residues, and we searched for binding modes that did not interact with these residues. From the 273 poses output in the docking study, we used Sidechain interaction in interaction fingerprints to narrow down the docking poses that interacted with the side chains of Arg66, Trp70, Ser147, Ser170, Glu297, and Ile416, which had a significant difference ( $P < 0.001$ ) in the relative binding results, and

did not interact with the side chains of Ser272 and Ser302 (Fig. 4). As a result, three poses were selected. These were all from the PDB 5FBH chain B docking study, and were the 31st, 37th, and 49th docking poses from the top, respectively (Fig. 4). For these poses, we performed molecular dynamics simulations three times at 120 ns to check whether the hydrogen bonds were maintained between the carboxyl group of upacicalcet and the main chain amine of Ser147, the side chain hydroxyl group of Ser147, and the main chain amine of Ser170, as well as between the alpha-amino group of upacicalcet and the side chain hydroxyl group of Ser170 and the main chain carbonyl of Ala168. When poses that maintained more than 30% of the interaction were considered as the appropriate binding mode, only the Rank 37 docking pose maintained the interaction in three molecular dynamics simulations (Fig. 4 and 8, Fig. S3).

Our proposed binding mode of CaSR to upacicalcet is shown in Fig. 9. The amino acid backbone of upacicalcet are similar to those of L-tryptophan and cyclomethyltryptophan. The carboxyl group of upacicalcet forms hydrogen bonds with the main chain amine of Ser147, the side chain hydroxyl group, and the main chain amine of Ser170, respectively, and the alpha-amino group of upacicalcet forms hydrogen bonds with the side chain hydroxyl group of Ser170 and the main chain carbonyl of Ala168, respectively. The side chain carboxyl group of Glu297, which formed hydrogen bonds with the amine of the indole ring in L-tryptophan, formed hydrogen bonds with each of the two amines of urea in the case of upacicalcet, and it also formed hydrogen bonds or ionic bonds with the alpha-amino group of upacicalcet. There are two specific interactions for upacicalcet: one is the sulfo group of upacicalcet, which forms hydrogen bonds with the side chain guanidyl group of Arg66, the main chain amine of Leu322, and also forms water-mediated hydrogen bonds with the main chain carbonyl of Phe320,



and the other is the carbonyl group of the urea of upacalcet, which forms water-mediated hydrogen bonds with the hydroxyl group of the side chain of Thr145. In addition, the benzene ring of upacalcet was closer to Ile416 than the benzene rings of L-tryptophan and cyclomethyltryptophan. We suspect that there is a hydrophobic interaction between the indole ring of the Trp70 side chain and the benzene ring of the upacalcet stacked in a T-shape ( $\pi$ -H stacking) and a hydrophobic interaction between the Ile416 side chain and the upacalcet.

The mutation causing I416A did not change the  $\text{Ca}^{2+}$ -responsiveness in the IP-1 assay but decreased the effect of upacalcet, compared with the wild type, and prominently decreased the relative binding ability. The hydrophobic interaction between Ile416 and upacalcet is likely to be stronger due to the closer intermolecular distance, compared with that for aromatic amino acids.

Trp70 is a residue that interacts with phosphorus as well as aromatic amino acids, and there is also a calcium binding site located nearby (Geng et al., 2016). In this study, alanine mutation significantly reduced the  $\text{Ca}^{2+}$  responsiveness of the CaSR. This suggests that Trp70 plays an important role in maintaining CaSR function. We think that the indole ring is one of the bulky side chains of alpha amino acids, so it may stabilize the structure of the ECD region, allowing it to be easily accessed by multiple ligands.

The functional groups of upacalcet seem to penetrate further into the pocket, especially the sulfo group and its interaction with Arg66 of CaSR. The main ligands for class C GPCRs such as CaSR are  $\alpha$ -amino acids. Alpha-amino acids fit into the amino acid binding pockets of many GPCRs and can cause dynamic conformational change. On the other hand, the amino acid binding sites of CaSR are larger than those of many GPCRs (Conigrave and Hampson, 2006a), so  $\alpha$ -amino acids alone are not sufficient to

induce conformational change. We believe that ligands that have a strong effect on CaSR need to interact with multiple residues that consist of the amino acid binding site. In fact, glutathione analogs, which are tripeptides, show stronger the maximum left shift of the  $\text{Ca}^{2+}$  concentration curve than amino acids ([Broadhead et al., 2011](#); [Amino et al., 2016](#)). In this study reveals that upacicalcet interacts with more residues compared to  $\alpha$ -amino acids. When the structure-activity relationship of upacicalcet was examined, the maximum left shift of the  $\text{Ca}^{2+}$  concentration curve was greatly reduced when the sulfo group was eliminated, suggesting that the interaction between the CaSR residue with the sulfo group extending from the aromatic ring of upacicalcet is important for the much stronger CaSR positive allosteric activity, compared with that seen for aromatic amino acids.

## Discussion

To define the binding mode of upacicalcet to CaSR, we hypothesized that upacicalcet works on the amino acid binding site of CaSR after focusing on two features: the chemical structure of upacicalcet is similar to that of amino acids, and upacicalcet is a positive allosteric modulator of CaSR. This study strongly suggests that upacicalcet acts on the amino acid binding site (Arg66, Trp70, Tyr145, Ser147, Ala168, Ser170, Glu297, Phe320, Leu322 and Ile416) of CaSR. Trp70, Glu297 and Ile416, which reportedly interact with L-tryptophan ([Geng et al., 2016](#)), all showed significant reductions in relative binding abilities as a result of alanine substitution. Among amino acids, L-tryptophan is known to have strong positive allosteric activity in the presence of  $\text{Ca}^{2+}$  against CaSR ([Conigrave et al., 2006b](#)). The hydrophobic interaction between the aromatic ring of the ligand and the hydrophobic residues of CaSR was considered to be important for binding, and a similar situation was suggested for upacicalcet. Furthermore, the interaction of the urea of upacicalcet with Glu297 of CaSR instead of the nitrogen atom of the indole ring of L-tryptophan is also likely to be important for binding. We evaluated the relative binding abilities of alanine substitutions at 3 amino acid residues, Arg66, Ser272, and Ser302, which were predicted to be of importance based on the results of a docking study between the ECD region of CaSR and upacicalcet. R66A resulted in a strong decrease in binding ability, although no decrease in binding ability was observed for S272A. Comparing the chemical structures of tryptophan and upacicalcet by overlapping the amino and carboxyl groups bound to the alpha carbon, upacicalcet is longer. The binding mode of upacicalcet is that the sulfo group extending from the benzene ring is located near the amino acid binding site of Arg66 (Fig. 9A). Tryptophan cannot interact with Arg66 because of its small molecular

size, and the interaction between the ligand and Arg66 is considered to be specific to upacalcet (Fig. 5C, Fig. 9A).

In this study, we considered that Ser302 does not contribute to the binding of upacalcet. It is possible that the test conditions affected the affinity of S302A-CaSR and upacalcet, given that Ser302 has been reported as a calcium binding site (Geng et al., 2016). To find the exact binding mode of upacalcet, it may be necessary to vary the concentration of calcium, phosphorus, etc., which have been reported as CaSR ligands. Among the calcimimetics, the  $IC_{50}$  of tryptophan (approx. 2mM) and evocalcet ( $9.47 \times 10^{-8}$  M) were shown in previous reports (Leach et al., 2016; Geng et al., 2016). Comparison of these results shows that upacalcet has a higher binding potency than tryptophan. The difference in binding potency between tryptophan and upacalcet might be attributed to more interacting residues in the amino acid binding site with upacalcet.

Amino acids are considered to act as a co-agonist for CaSR in cooperation with  $Ca^{2+}$ . Aromatic amino acids that can interact more with CaSR are considered to be the primary players *in vivo*. Upacalcet is expected to function in a manner similar to that of amino acids. Surprisingly, upacalcet showed a strong  $Ca^{2+}$  response recovery in an IP-1 assay even in the presence of mutant CaSR proteins (S147A, S170A and E297A), the  $Ca^{2+}$  responses of which are greatly decreased. This result may be due to the interaction of the sulfo group, benzene ring, and urea skeleton of upacalcet with the residues constituting the amino acid binding site (Arg66, Trp70, Ile416, and Glu297, respectively), thereby compensating for the decrease in relative binding caused by mutations targeting some of the important amino acid binding sites.

These results strongly suggest that upacalcet is a “novel” SHPT drug that binds to

the amino acid binding site, unlike conventional drugs such as cinacalcet and etelcalcetide. As SNPs of CaSR have been reported to affect the pathophysiology of hemodialysis patients and the therapeutic effect, upacalcet might be expected to be a new option for patients who do not respond well to conventional drugs (Ngamkam et al., 2021; Grzegorzewska et al., 2016).

CaSR has multiple calcium binding sites, and the affinity of each binding site for  $\text{Ca}^{2+}$  is thought to change depending on the activation state of the receptor (Geng et al., 2016). Furthermore, the affinity of amino acids for CaSR is thought to depend on the extracellular  $\text{Ca}^{2+}$  concentration (Geng et al., 2016). Upacalcet might have a relatively low risk of adverse effects such as hypocalcemia, since it does not act excessively on CaSR and its affinity may change depending on the extracellular  $\text{Ca}^{2+}$  concentration. In fact, an *in vitro* validation of upacalcet has confirmed that it exerts a pure positive allosteric effect that does not affect the  $E_{\max}$  and increases  $\text{Ca}^{2+}$  sensitivity only at low  $\text{Ca}^{2+}$  concentrations. One group has shown that L-tryptophan alone does not activate CaSR, but that the binding of L-tryptophan induces the closure of the Venus flytrap domain of CaSR, bringing the receptor to an intermediate active state, based on a single-particle cryo structural approach (Ling et al., 2021). In clinical study, the risk of hypocalcemia is often reported with etelcalcetide, which binds to the extracellular region (Bushinsky et al., 2020), but the incidence of hypocalcemia was low in the clinical trials of upacalcet (Hoy SH., 2021). The difference in the effects of etelcalcetide and upacalcet on CaSR *in vitro* (agonist or purely positive allosteric effect) is consistent with the results of clinical studies. These information indicate that upacalcet acts to “wake up” the CaSR in a diminished or inactivated state, and it could be a safe drug for “awakened” CaSR, since there is a low risk of causing a “runaway”

state of activation.

Arg66 and Trp70 have been reported as anion-binding residues in upacicalcet, and anions such as  $\text{PO}_4^{3-}$  and  $\text{SO}_4^{2-}$  are considered to be among the molecules that affect the conformation of CaSR ([Geng et al., 2016](#); [Centeno et al., 2019](#)). In particular, phosphate ions stabilize the inactivated state of CaSR, suggesting that CaSR function is impaired in patients with hyperphosphatemia ([Centeno et al., 2019](#)). Recently, CaSR has been reported to function as a cation sensor for calcium, magnesium, and cadmium as well as an anion sensor for phosphate ion and others ([Centeno et al., 2019](#)). One of the important pathologies of SHPT is ectopic calcification, which is caused by the formation of insoluble salts of calcium and phosphate ions in the blood. In patients with hyperphosphatemia, the CaSR function is impaired, and the calcium sensor does not work properly, which may lead to excessive PTH secretion ([Cunningham et al., 2011](#); [Go et al., 2004](#)). In the inactivated state, the ECD region of CaSR has a characteristic conformation, compared with that in the activated state, and the amino acid binding sites are thought to be wide open ([Ling et al., 2021](#)). Therefore, in the inactivated state, the amino acid binding site of CaSR might be more approachable, facilitating the binding of upacicalcet. In addition, the interaction of upacicalcet with anion-binding residues such as Arg66 and Trp70 is expected to release the inactivated state of CaSR and to promote a transition to the activated state. Upacicalcet is also expected to suppress these negative spirals by approaching the CaSR, which is impaired due to high phosphorus and high calcium levels. In the future, clarification of the interaction between upacicalcet and CaSR ligands, such as anions, may help to consider the clinical details of the drug's effect.

In conclusion, upacalcet shows a strong positive allosteric effect by interacting with the amino acid binding site of CaSR. The binding mode of upacalcet involves interactions with several residues that constitute the amino acid binding site of CaSR. In addition to residues participating in known interactions between aromatic amino acids and CaSR, the interaction residues possessed only by upacalcet are thought to be responsible for its much higher positive allosteric activity, relative to that of amino acids. Since this mechanism differs from those of conventional drugs, upacalcet can be considered as a “novel” SHPT drug that acts on the amino acid binding site of CaSR.

### **Acknowledgements**

We thank Nahika Tanaka and Minami Inagaki for the kind support to conduct the *in vitro* experiments in this study.

### **Author contributions**

Participated in research design: Sato, Murakami, Nishimura, Goto, and Takahashi

Conducted experiments: Sato, Murakami, Horii, and Iwai

Performed data analysis: Sato, Murakami, and Horii

Wrote or contributed to manuscript writing: Sato, Murakami, and Goto

## References

Alexander ST, Hunter T, Walter S, Dong J, Maclean D, Baruch A, Subramanian R and Tomlinson JE (2015). Critical Cysteine Residues in Both the Calcium-Sensing Receptor and the Allosteric Activator AMG 416 Underlie the Mechanism of Action. *Mol Pharmacol* **88**: 853-865.

Amino Y, Nakazawa M, Kaneko M, Miyaki T, Miyamura N, Maruyama Y, and Eto Y (2016). Structure-CaSR-Activity Relation of Kokumi  $\gamma$ -Glutamyl Peptides. *Chem Pharm Bull* **64**: 1181-1189.

Bowers KJ, Chow DE, Xu H, Dror RO, Eastwood MP, Gregersen BA, Klepeis JL, Kolossvary I, Moraes MA, Sacerdoti FD, Salmon JK, Shan Y and Shaw DE (2006). Scalable algorithms for molecular dynamics simulations on commodity clusters. Proceedings of the ACM/IEEE Conference on Supercomputing (SC06) Tampa, Florida, USA.

Broadhead GK, Mun H, Avlani VA, Jourdon O, Church WB, Christopoulos A, Delbridge L and Conigrave AD (2011). Allosteric modulation of the calcium-sensing receptor by gamma-glutamyl peptides: inhibition of PTH secretion, suppression of intracellular cAMP levels, and a common mechanism of action with L-amino acids. *J Biol Chem* **286**: 8786-8797.

Bushinsky DA, Chertow GM, Cheng S, Deng H, Kopyt N, Martin KJ, Rastogi A,



Ureña-Torres P, Vervloet M, Block GA (2020). One-year safety and efficacy of intravenous etelcalcetide in patients on hemodialysis with secondary hyperparathyroidism. *Nephrol Dial Transplant* 35: 1769-1778.

Centeno PP, Herberger A, Mun HC, Tu C, Nemeth EF, Chang W, Conigrave AD and Ward DT (2019). Phosphate acts directly on the calcium-sensing receptor to stimulate parathyroid hormone secretion. *Nat Commun* 10: 4693.

Conigrave AD, Franks AH, Brown EM and Quinn SJ (2002). L-Amino acid sensing by the calcium-sensing receptor: a general mechanism for coupling protein and calcium metabolism? *Eur J Clin Nutr* 56: 1072-1080.

Conigrave AD, Mun H, Delbridge L, Quinn SJ, Wilkinson M, and Brown EM (2004). L-Amino Acids Regulate Parathyroid Hormone Secretion. *J Biol Chem* 279: 38151-38159.

Conigrave AD and Hampson DR (2006a). Broad-spectrum L-amino acid sensing by class 3 G-protein-coupled receptors. *Trends Endocrinol Metab* 10: 398-407.

Conigrave AD, Quinn SJ, and Brown EM (2006b). L-Amino acid sensing by the extracellular  $\text{Ca}^{2+}$ -sensing receptor. *Proc Natl Acad Sci U S A* 97: 4814-4819.

Cunningham J, Locatelli F and Rodriguez M (2011). Secondary hyperparathyroidism:

pathogenesis, disease progression, and therapeutic options. *Clin J Am Soc Nephrol* **6**: 913-921.

Deng Z, Chuaqui C and Singh J (2004). Structural interaction fingerprint (SIFt): a novel method for analyzing three-dimensional protein-ligand binding interactions. *J Med Chem* **47**: 337-344.

D'Souza-Li L (2006). The calcium-sensing receptor and related diseases. *Arg Bras Endocrinol Metabol* **50**: 628-39.

Friesner RA, Banks JL, Murphy RB, Halgren TA, Klicic JJ, Mainz DT, Repasky MP, Knoll EH, Shelley M, Perry JK, Shaw DE and Francis P (2004). Glide: a new approach for rapid, accurate docking and scoring. 1. Method and assessment of docking accuracy. *J Med Chem* **47**: 1739-1749.

Geng Y, Mosyak L, Kurinov I, Zuo H, Sturchler E, Cheng TC, Subramanyam P, Brown AP, Brennan SC, Mun H, Bush M, Chen Y, Nguyen TX, Cao B, Chang DD, Quick M, Conigrave AD, Colecraft HM, McDonald P, Fan QR (2016). Structural mechanism of ligand activation in human calcium-sensing receptor. *Elife* **5**: e13662.

Go AS, Chertow GM, Fan D, McCulloch CE and Hsu C (2004). Chronic kidney disease and the risks of death, cardiovascular events, and hospitalization. *N Engl J Med* **13**: 1296-305.

Grzegorzewska AE, Paciorkowski M, Mostowska A, Frycz B, Warchoń W, Stolarek I, Figlerowicz Marek and Jagodziński PP (2016). Associations of the calcium-sensing receptor gene CASR rs7652589 SNP with nephrolithiasis and secondary hyperparathyroidism in haemodialysis patients. *Sci Rep* **6**: 35188.

Hoy SM (2021). Upacalcet: First Approval. *Drugs* **81**: 1593-1596.

Jacobsen SE, Gether U, and Bräuner-Osborne H (2017). Investigating the molecular mechanism of positive and negative allosteric modulators in the calcium-sensing receptor dimer. *Sci Rep* **7**: 46355.

Jorgensen WL, Chandrasekhar J, Madura JD, Impey RW and Klein ML (1983). Comparison of simple potential functions for simulating liquid water. *J Chem Phys* **79**: 926-935.

Lau WL, Obi Y and Kalantar-Zadeh K (2018). Parathyroidectomy in the Management of Secondary Hyperparathyroidism. *Clin J Am Soc Nephrol* **6**: 952-961.

Leach K, Gregory KJ, Kufareva I, Khajehali E, Cook AE, Abagyan R, Conigrave AD, Sexton PM and Christopoulos A (2016). Towards a structural understanding of allosteric drugs at the human calcium-sensing receptor. *Cell Res* **26**: 574-592.

Ling S, Shi P, Liu S, Meng X, Zhou Y, Sun W, Chang S, Zhang X, Zhang L, Shi C, Sun Demeng, Liu L and Tian C (2021). Structural mechanism of cooperative activation of the human calcium-sensing receptor by  $\text{Ca}^{2+}$  ions and L-tryptophan. *Cell Res* **31**: 383-394.

Miyazaki H, Ikeda Y, Sakurai O, Miyake T, Tsubota R, Okabe J, Kuroda M, Hisada Y, Yanagida T, Yoneda H, Tsukumo Y, Tokunaga S, kawata T, Ohashi R, Fukuda H, Kojima K, Kannami A, Kifuji T, Sato N, Idei A, Iguchi T, Sakairi T and Moritani Y (2018). Discovery of evocalcet, a next-generation calcium-sensing receptor agonist for the treatment of hyperparathyroidism. *Bioorg Med Chem Lett* **28**: 2055-2060.

Nemeth EF, Heaton WH, Miller M, Fox J, Balandrin MF, Van Wagenen BC, Colloton M, Karbon W, Scherrer J, Shatzen E, Rishton G, Scully S, Qi M, Harris R, Lacey D and Martin D (2004). Pharmacodynamics of the Type II Calcimimetic Compound Cinacalcet HCl. *J Pharmacol Exp Ther* **308**: 627-635.

Ngamkam J, Vadcharavivad S, Areepium N, Auamnoy T, Takkavatakarn K, Katavetin P, Tiranathanagul K, Praditpornsilpa K, Eiam-Ong S and Susantitaphong P (2021). The impact of CASR A990G polymorphism in response to cinacalcet treatment in hemodialysis patients with secondary hyperparathyroidism. *Sci Rep* **11**: 18006.

Roos K, Wu C, Damm W, Reboul M, Stevenson JM, Lu C, Dahlgren MK, Mondal S, Chen W, Wang L, Abel R, Friesner RA and Harder ED (2019). OPLS3e: Extending

Force Field Coverage for Drug-Like Small Molecules. *J Chem Theory Comput* **15**:1863-1874.

Sastry GM, Adzhigirey M, Day T, Annabhimoju R and Sherman W (2013). Protein and ligand preparation: parameters, protocols, and influence on virtual screening enrichments. *J Comput Aided Mol Des* **27**: 221-234.

Sherman W, Day T, Jacobson MP, Friesner RA, and Farid R (2006). Novel procedure for modeling ligand/receptor induced fit effects. *J Med Chem* **49**: 534-553.

Silve C, Petrel C, Leroy C, Bruel H, Mallet E, Rognan D, and Ruat M (2005). Delineating a Ca<sup>2+</sup> Binding Pocket within the Venus Flytrap Module of the Human Calcium-sensing Receptor. *J Biol Chem* **280**: 37917-37923.

Singh J, Deng Z, Narale G and Chuaqui C (2006). Structural Interaction Fingerprints: A New Approach to Organizing, Mining, Analyzing, and Designing Protein-Small Molecule Complexes. *Chem Biol Drug Des* **67**: 5-12.

Ueda Y, Yonemitsu M, Tsubuku T, Sakaguchi M and Miyajima R (1997). Flavor characteristics of glutathione in raw and cooked foodstuffs. *Biosci Biotechnol Biochem* **61**:1977-80.

Walter S, Baruch A, Dong J, Tomlinson JE, Alexander ST, Janes J, Hunter T, Yin Q,

Maclean D, Bell G, Mendel DB, Johnson RM and Karim F (2013). Pharmacology of AMG 416 (Velcalcetide), a Novel Peptide Agonist of the Calcium-Sensing Receptor, for the Treatment of Secondary Hyperparathyroidism in Hemodialysis Patients. *J Pharmacol Exp Ther* 346: 229-240.

Zhang C, Zhang T, Zou J, Miller CL, Gorkhali R, Yang J, Schilmiller A, Wang S, Huang K, Brown EM, Moremen KW, Hu J and Yang JJ (2016). Structural basis for regulation of human calcium-sensing receptor by magnesium ions and an unexpected tryptophan derivative co-agonist. *Sci Adv* 2: e1600241.

Zhang JY, Kowal DM, Nawoschik SP, Dunlop J, Pausch MH and Peri R (2010). Development of an improved IP(1) assay for the characterization of 5-HT(2C) receptor ligands. *Assay Drug Dev Technol* 8: 106-113.

Zhang Z, Qiu W, Quinn SJ, Conigrave AD, Brown EM and Bai M (2002). Three Adjacent Serines in the Extracellular Domains of the CaR Are Required for L-Amino Acid-mediated Potentiation of Receptor Function. *J Biol Chem* 277: 33727-33735.

## Footnotes

This work received no external funding.

The authors declare that they have no conflicts of interest with the contents of this article.

## Figure legends

### **Fig. 1 Comparison of the molecular structures of calcimimetics**

(A) Molecular structures of L-tryptophan, cyclomethyltryptophan, upacicalcet and glutathione analogs with positive allosteric activities toward CaSR.

(B) Molecular structures of cinacalcet and etelcalcetide, two drugs approved for the treatment of SHPT.

### **Fig. 2 Positive allosteric activity of upacicalcet on HEK-293T cells stably expressing human calcium-sensing receptor as measured by intracellular calcium mobilization**

Concentration-dependent orthosteric agonist activity of 0.1-1.5 mM  $\text{Ca}^{2+}$  in the presence of  $\text{Ca}^{2+}$  alone (closed circle), 10 nM of upacicalcet (closed square), or 1000 nM of upacicalcet (closed triangle). Each plot was derived from the relative fluorescence unit (RFU)-fold change relative to the baseline (before the application of  $\text{Ca}^{2+}$ ). The data are presented as the mean  $\pm$  S.D. of three experiments.

### **Fig. 3 Ligand competitive study of upacicalcet with L-tryptophan or cinacalcet using a scintillation proximity assay and membrane proteins of HEK-293T cells stably expressing human calcium-sensing receptor**

(A) Confirmation of ligand-receptor interaction by SPA beads emission. Concentration-dependent inhibition of cold upacicalcet on the interaction between [ $^3\text{H}$ ]-upacicalcet and CaSR. Counts are shown for CaSR-expressing (closed square) or non-expressing (open square) HEK-293T cell membrane proteins in the presence of

[<sup>3</sup>H]-upacalcet, 15,000 dpm. **(B)** Concentration-dependent inhibition of L-tryptophan on the interaction between [<sup>3</sup>H]-upacalcet and CaSR. Counts are shown for CaSR-expressing (closed circle) or non-expressing (open circle) HEK-293T cell membrane proteins. **(C)** Cinacalcet does not affect the interaction between [<sup>3</sup>H]-upacalcet and CaSR. Counts are shown for CaSR-expressing (closed square) or non-expressing (open square) HEK-293T cell membrane proteins. The data are presented as the mean ± S.D. of three independent experiments measured in triplicate.

#### **Fig. 4 Flow chart of *in silico* procedures**

Upacalcet was first docked into the amino acid binding site of six CaSR structures using the induced fit docking, then the interaction fingerprint analysis was performed for all output docking poses. The interaction fingerprints of the sidechain interaction were used to confirm the high frequency of amino acid residues interacted with upacalcet in order to select the mutation site of CaSR for the relative binding ability assay. All docking poses were filtered using the interaction fingerprints of the sidechain interaction to detect docking poses that corresponded to the relative binding results of upacalcet to various mutant CaSR. Finally, molecular dynamics simulation was used to determine the binding mode that maintains the hydrogen bonds between the amino acid backbone of upacalcet and the CaSR as well as L-tryptophan or cyclomethyltryptophan.

#### **Fig. 5 The amino acid binding site of CaSR to which upacalcet is estimated to bind**

The estimated binding site of upacalcet is shown for the crystal structure of the ECD



region (PDB 5K5S chain A). The 8 residues of CaSR that were evaluated for binding ability and Ala168 are shown in stick representation. The binding mode of tryptophan is shown in cyan as a reference. H-bond interactions are represented as yellow dotted lines. (A) Overall view of the ECD region (B) Front view of the amino acid binding site (C) Bottom view of the amino acid binding site.

**Fig. 6 Evaluation of relative binding ability of upacalcet to HEK-293T cell membrane proteins expressing wild-type or mutant calcium-sensing receptors using a scintillation proximity assay**

(A) Confirmation of each receptor expression level using whole proteins of HEK-293 cells transfected with plasmids encoding full-length wild-type and mutant calcium-sensing receptors using a western blot analysis. Ten micrograms of protein were applied to each lane. Detected band at around 130 kDa: CaSR. (B) Relative binding results of upacalcet to various mutant calcium-sensing receptors when the binding ability of upacalcet to the wild-type calcium-sensing receptor was 100%. Black, WT; gray, C482Y and E837A; dots, S147A and S170A; slashes, W70A, E297A and I416A; stripes, R66A, S272A and S302A; white, HEK. All tests were performed three times and measured in triplicate (data are shown as the mean  $\pm$  S.D.). The statistical analysis in the relative binding affinities of upacalcet to each mutant CaSR and vs. wild-type CaSR was performed using the Student t-test by a one-way ANOVA followed by the Dunnett's multiple comparison. (\* $P < 0.05$ , \*\*\* $P < 0.001$ ).

**Fig. 7 Effect of the mutation of CaSR protein on IP-1 accumulation of transiently CaSR expressing HEK-293T cells in the presence of upacalcet**

(A) Positive allosteric activity of upacicalcet on wild-type CaSR.  $\text{Ca}^{2+}$  concentration-dependent IP-1 accumulation is shown (open circle,  $\text{Ca}^{2+}$  only; closed circle, in the presence of 100  $\mu\text{M}$  upacicalcet). (B–E) Comparison of IP-1 accumulation between wild-type and mutant CaSR in the presence of 100  $\mu\text{M}$  upacicalcet. The percentage for each mutant CaSR protein based on an  $E_{\text{max}}$  of 100% for IP-1 accumulation in the wild type is shown. (B) closed circle, WT; closed triangle, C482Y; closed square, E837A (C) closed circle, WT; closed triangle, S147A; closed square, S170A; closed rhombus, E297A (D) closed circle, WT; closed triangle, W70A; closed square, I416A (E) closed circle, WT; closed triangle, R66A; closed square, S302A closed rhombus, S272A. The data are presented as the mean  $\pm$  S.D. of three independent experiments measured in duplicate.

**Fig. 8 Estimation of upacicalcet binding mode based on molecular dynamics simulation (simulation 1)**

2D summary of interaction analysis results of IFD rank 37 of PDB 5FBH chain B during 120 ns of molecular dynamics simulations. The interaction pairs that occur during more than 30% of the simulation time are included (top). The RMSD of protein and ligand relative to the starting complexes during 120 ns of molecular dynamics trajectory (bottom).

**Fig. 9 Binding mode of upacicalcet to CaSR**

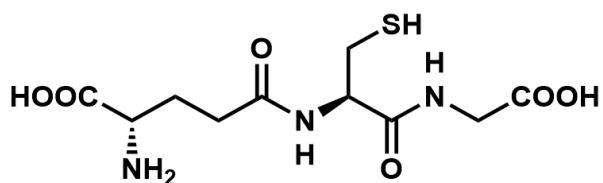
The figure shows the final snapshot of molecular dynamics simulation 2 for IFD rank 37 of PDB 5FBH chain B. 3D and 2D representation of the putative binding mode of upacicalcet to CaSR by molecular dynamics simulation. (A) H-bond interactions are

represented as yellow dotted lines. **(B)** Solid black line, C alpha backbone; red, negative charge; blue, positive charge; green, hydrophobic. The thick color line marks the molecular surface of the protein.

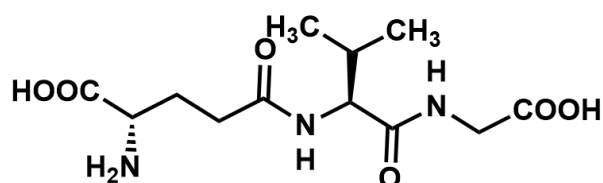
**Table 1.** Result of ligand-protein interaction analysis of docking poses

Amino acid residue of CaSR	Frequency of interaction	Interaction with L-Trp
Asn64	66	
Arg66	88	
Trp70	74	presence
Asn102	14	
Thr145	37	
Ser147	89	presence
Ala168	22	
Ser170	89	presence
Ile187	2	
Tyr218	89	presence
Ser272	63	
Asp275	1	
Glu297	32	presence
Ala298	84	
Ser301	48	
Ser302	83	
Ser303	16	
Ala321	4	
Arg415	12	
Ile416	50	

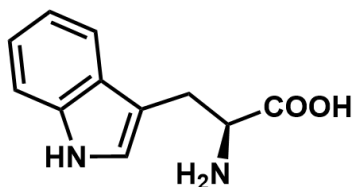
**A**



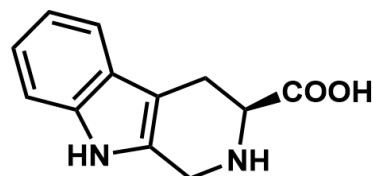
Glutathione (L-γ-glutamyl-L-cysteinyl-glycine)



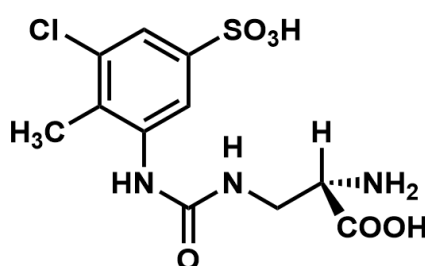
γ-EVG (L-γ-Glutamyl-L-Valyl-Glycine)



L-Tryptophan

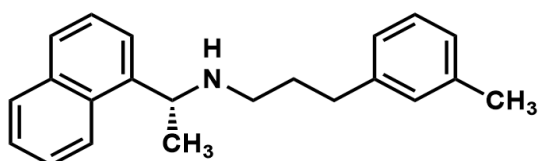


Cyclomethyltryptophan (TNCA)

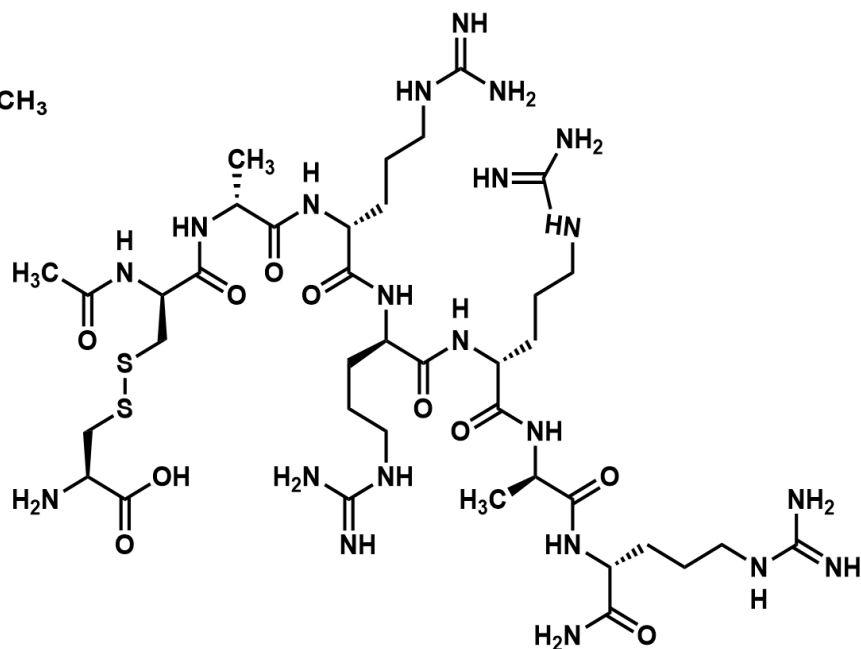


Upacicalcet

**B**



Cinacalcet



Eelcalcetide

**Figure 1**

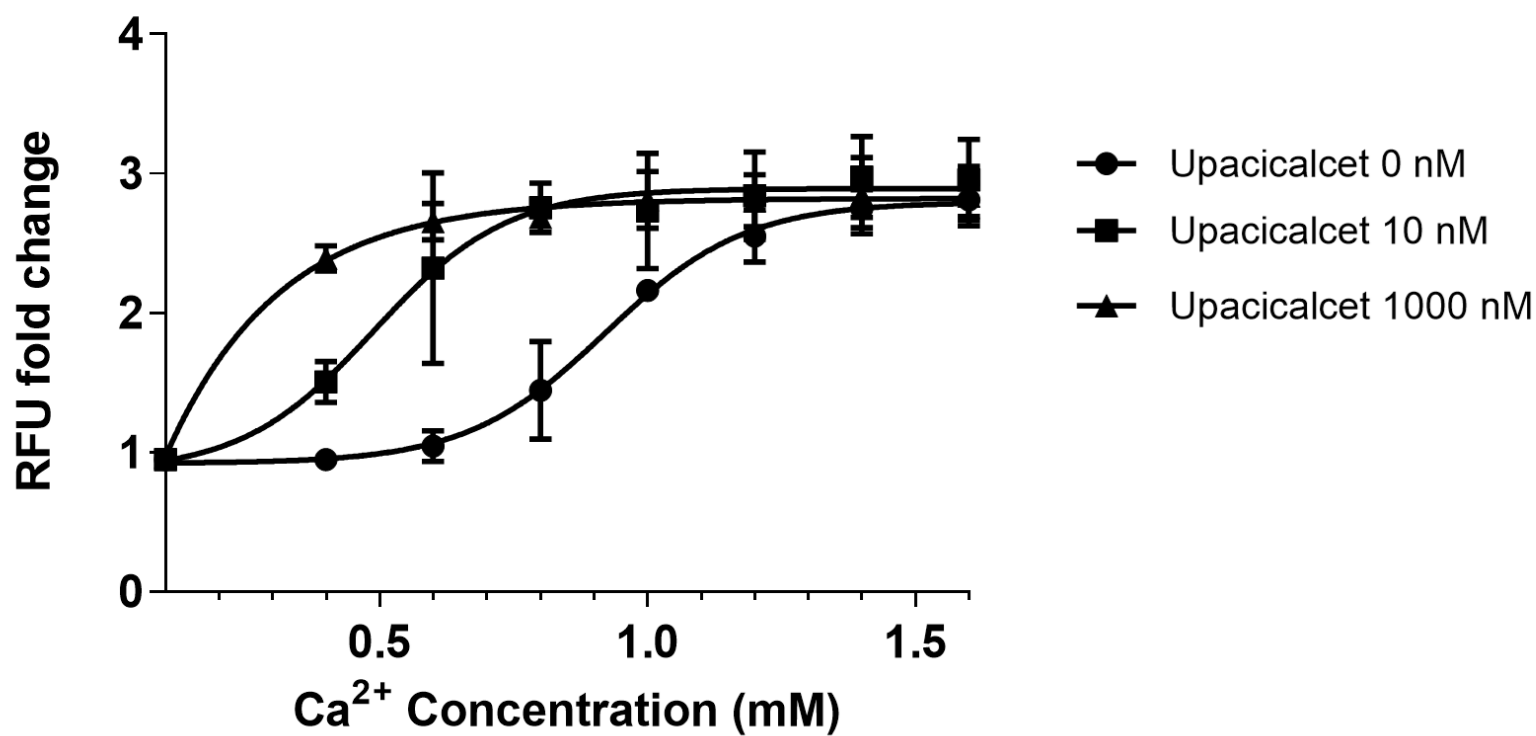


**Figure 2**

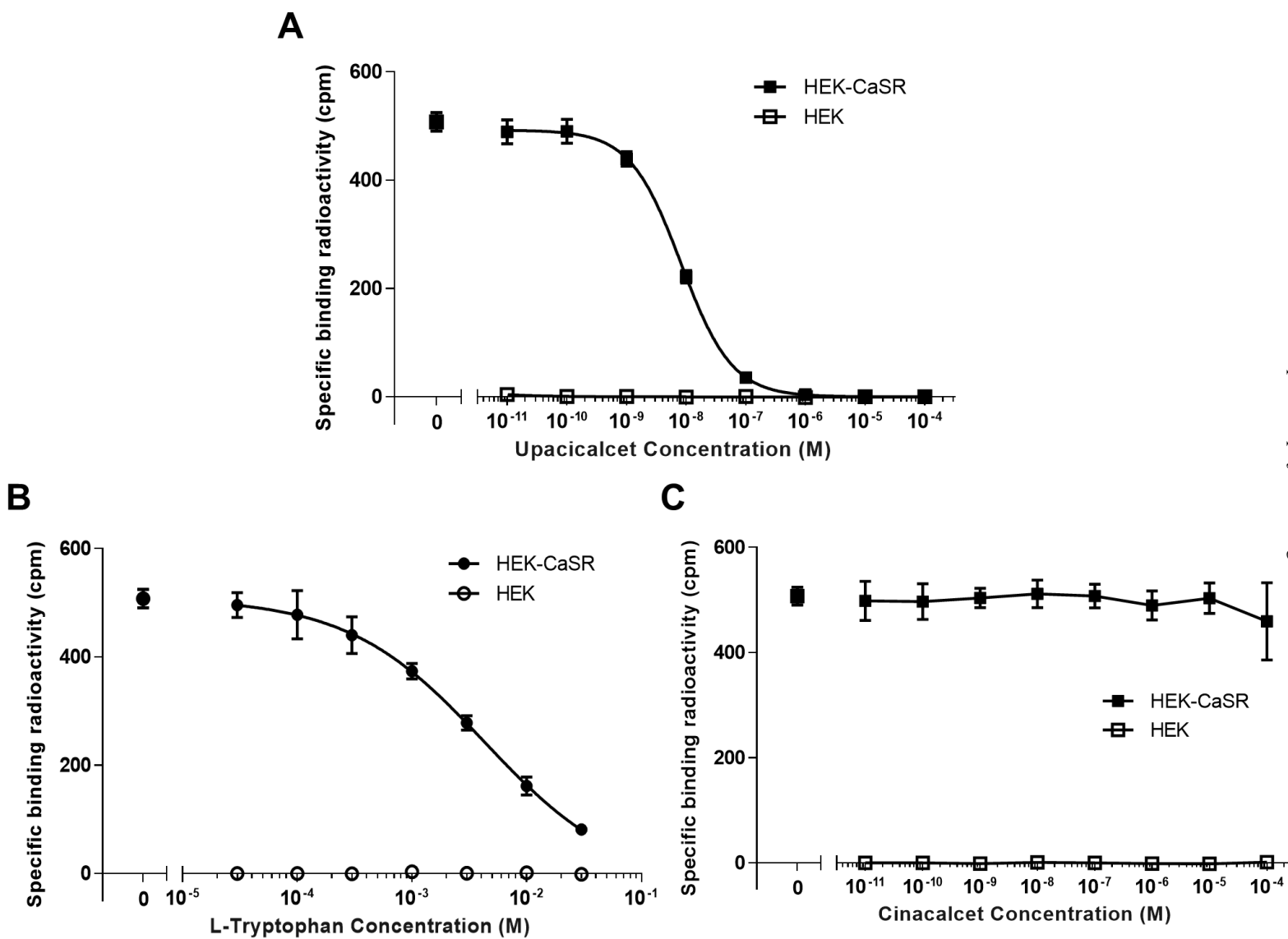


**Figure 3**

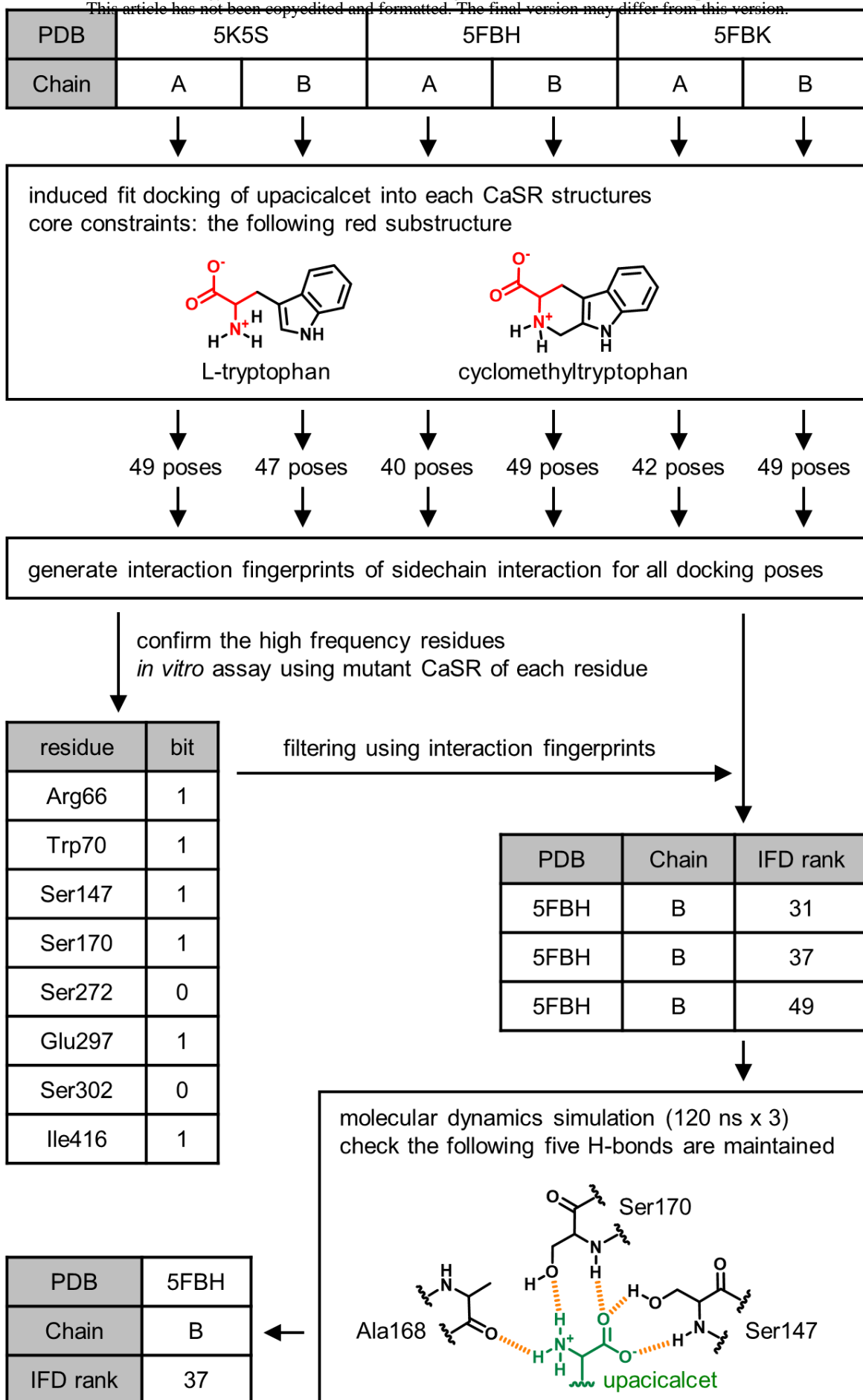


**Figure 4**



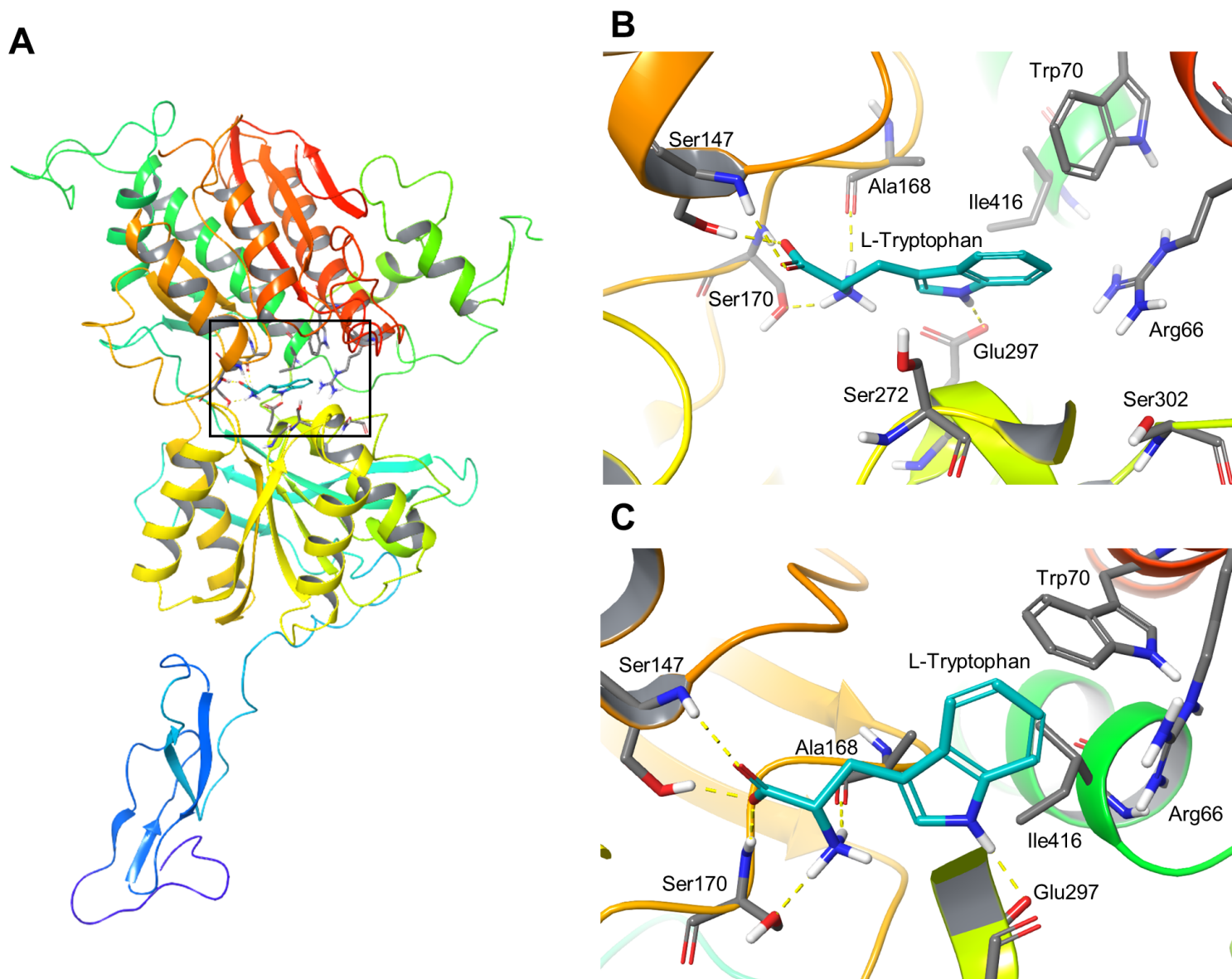


**Figure 5**

**A**



**B**

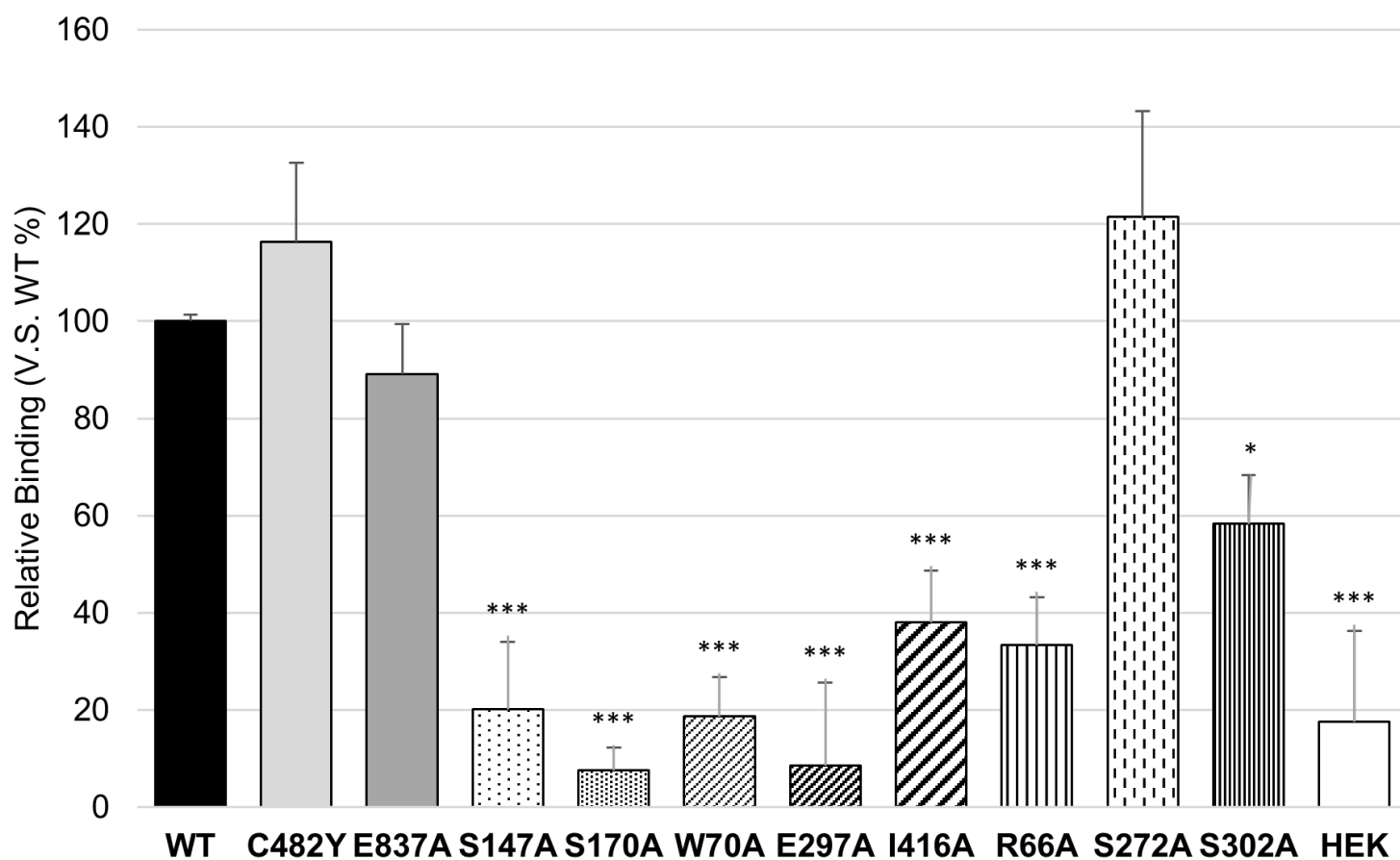


**Figure 6**

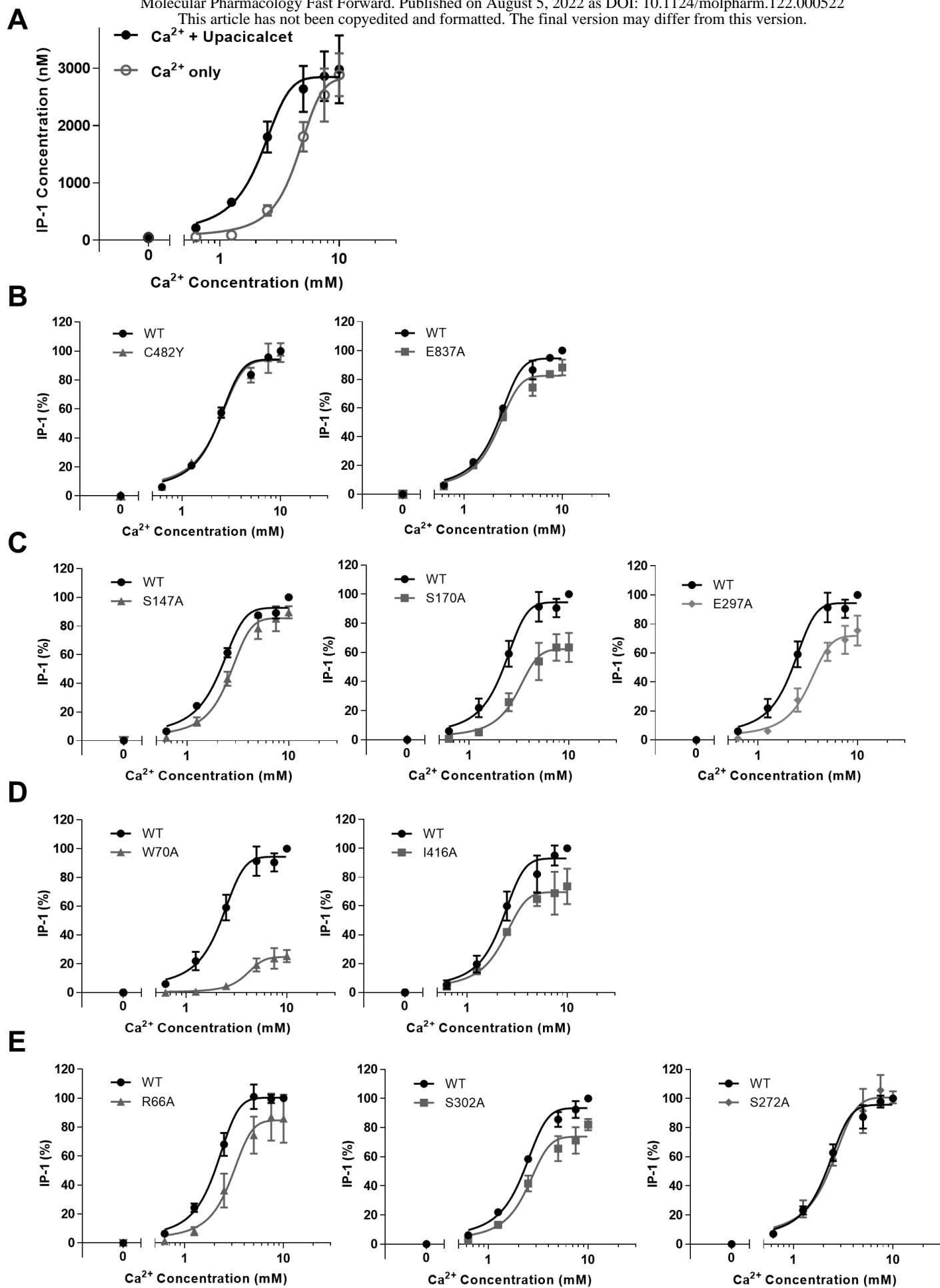


**Figure 7**

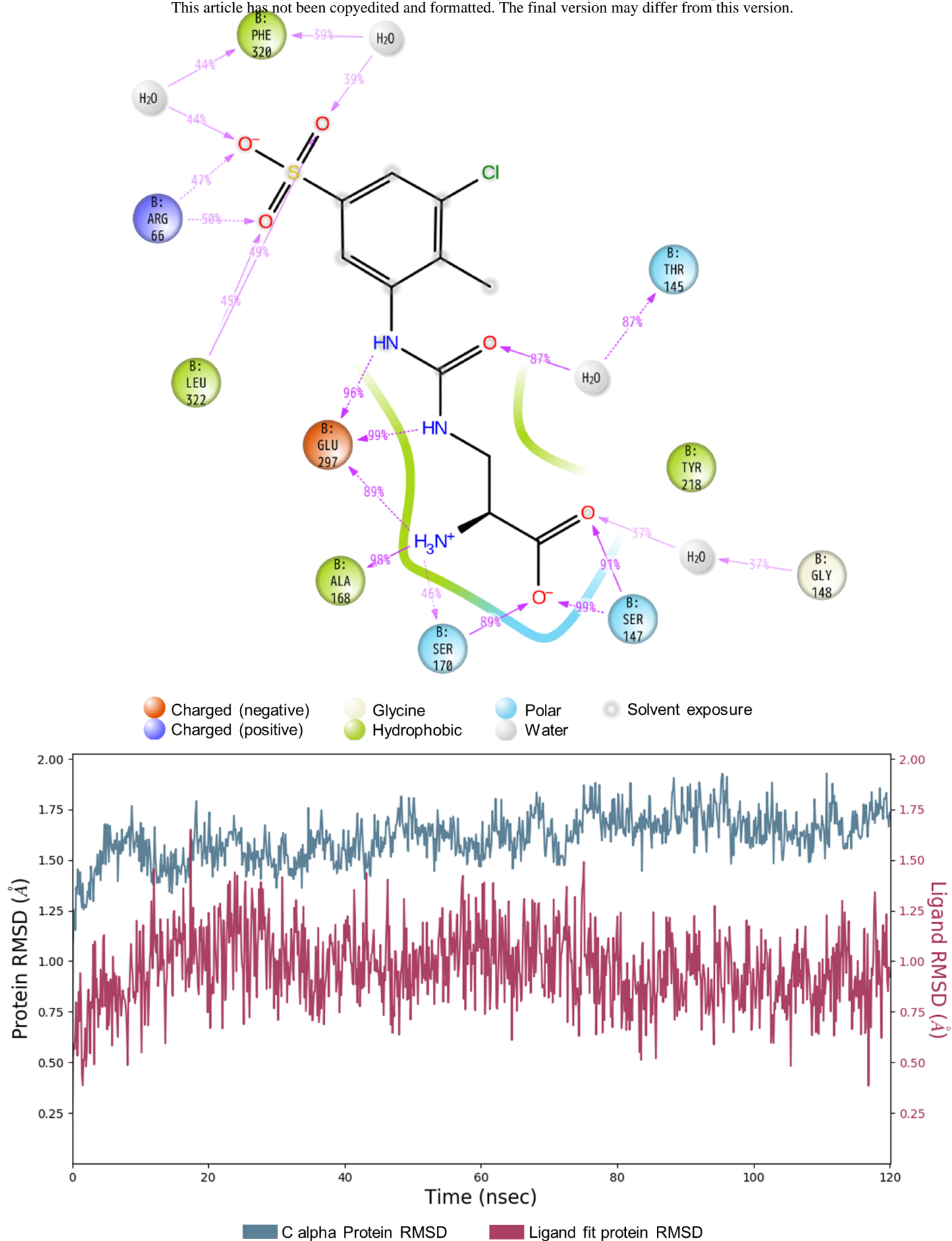
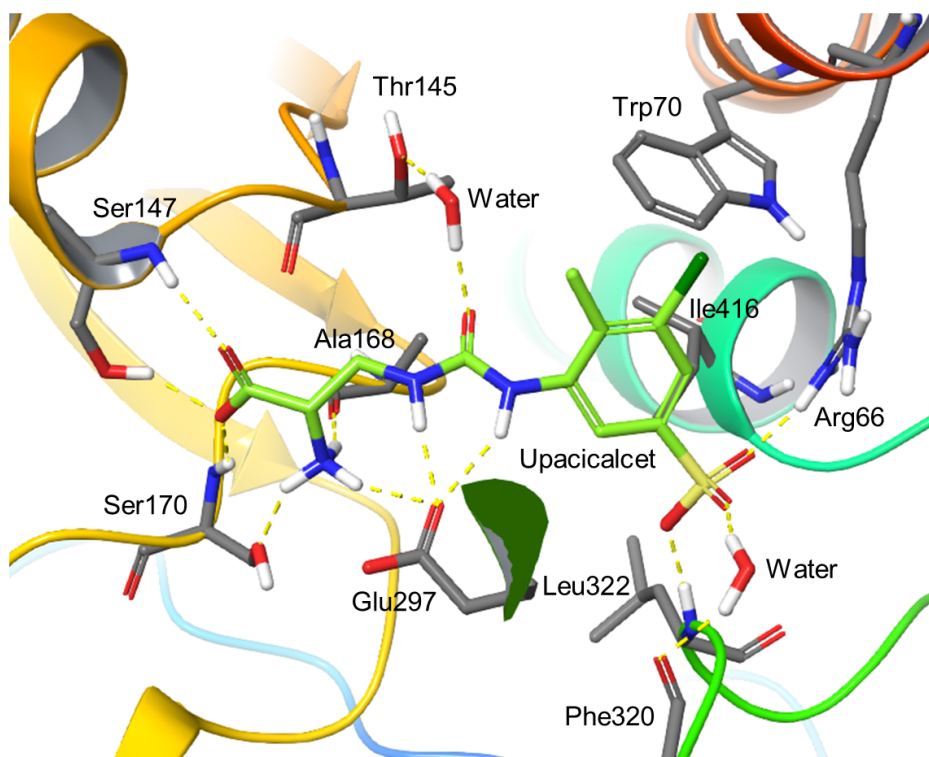


**Figure 8**

**A**



**B**

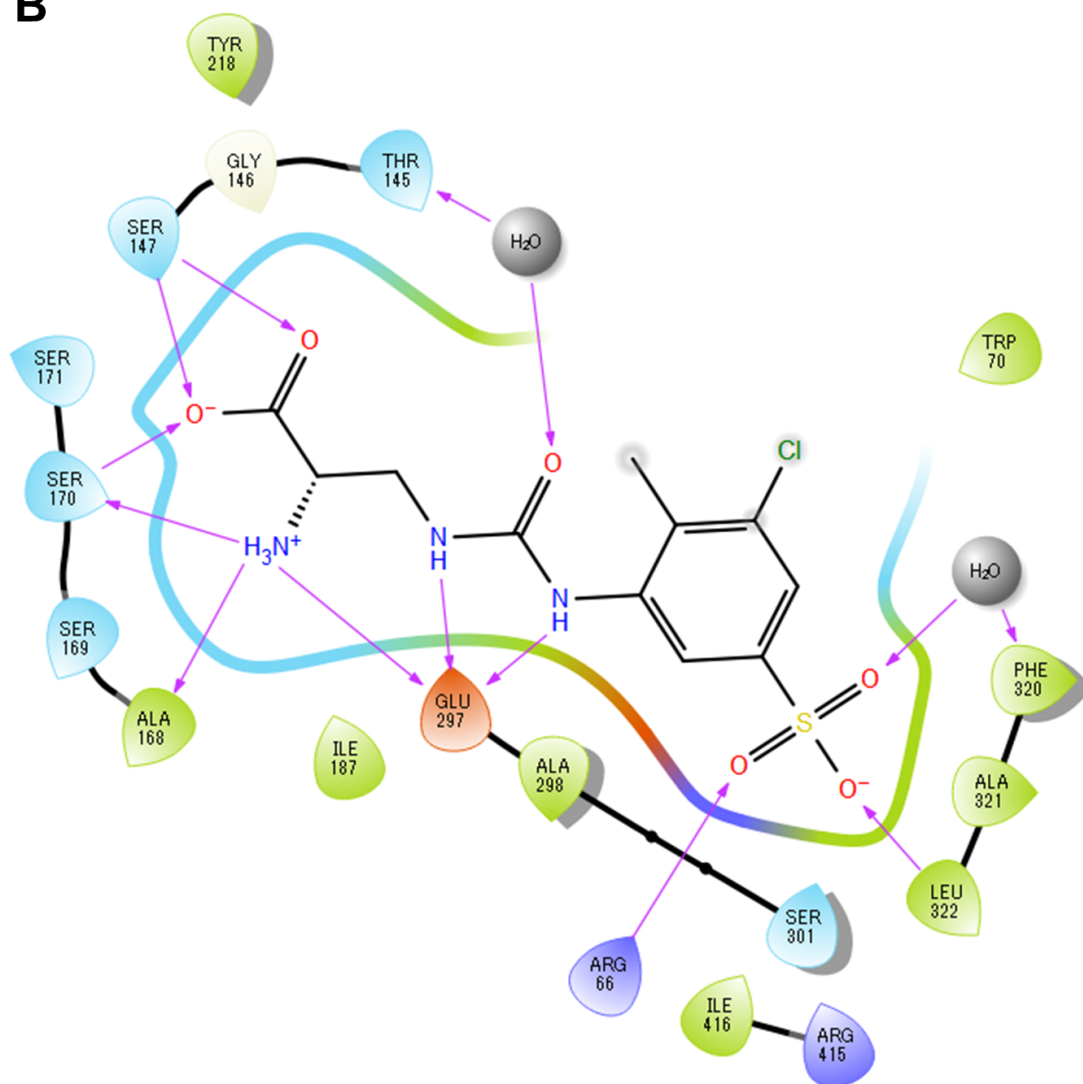


**Figure 9**

## Supplemental Information

**Upacicalcet is a novel secondary hyperparathyroidism drug that targets the amino acid binding site of calcium-sensing receptor**

Hirofumi Sato, Sei Murakami, Yusuke Horii, Go Nishimura, Ryosuke Iwai, Moritaka Goto, and Naoki Takahashi

Pharmaceuticals Research Laboratories, Sanwa Kagaku Kenkyusho Co., Ltd., Mie, Japan

**Table S1 Competitive binding study result of cold upacicalcet, L-tryptophan and cinacalcet using a scintillation proximity assay**

<i>Parameter</i>	<i>L-Tryptophan</i>	<i>Upacicalcet</i>
<i>Best-fit values</i>		
<i>Bottom</i>	-22.5	0.1329
<i>Top</i>	509.1	492.4
<i>LogIC50</i>	-2.37	-8.086
<i>HillSlope</i>	-0.7305	-1.016
<i>IC50</i>	<b>0.00427</b>	<b>8.2E-09</b>
<i>Std. Error</i>		
<i>Bottom</i>	69.87	3.938
<i>Top</i>	19.14	5.152
<i>LogIC50</i>	0.1657	0.02636
<i>HillSlope</i>	0.158	0.06388
<i>95% Confidence Intervals</i>		
<i>Bottom</i>	-169.9 to 124.9	-8.081 to 8.346
<i>Top</i>	468.7 to 549.5	481.7 to 503.2
<i>LogIC50</i>	-2.719 to -2.020	-8.141 to -8.031
<i>HillSlope</i>	-1.064 to -0.3972	-1.150 to -0.8831
<i>IC50</i>	0.001909 to 0.009551	7.225e-009 to 9.307e-009
<i>Goodness of Fit</i>		
<i>Degrees of Freedom</i>	17	20
<i>R square</i>	0.9811	0.9975
<i>Absolute Sum of Squares</i>	9026	2757
<i>Sy.x</i>	23.04	11.74

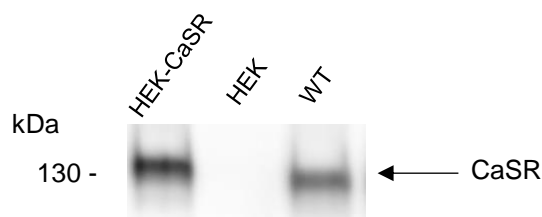
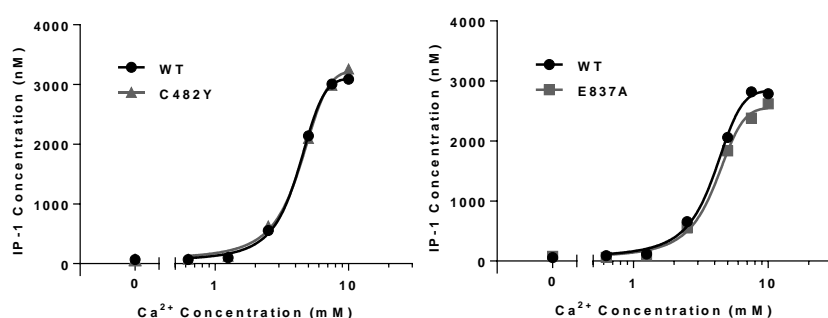


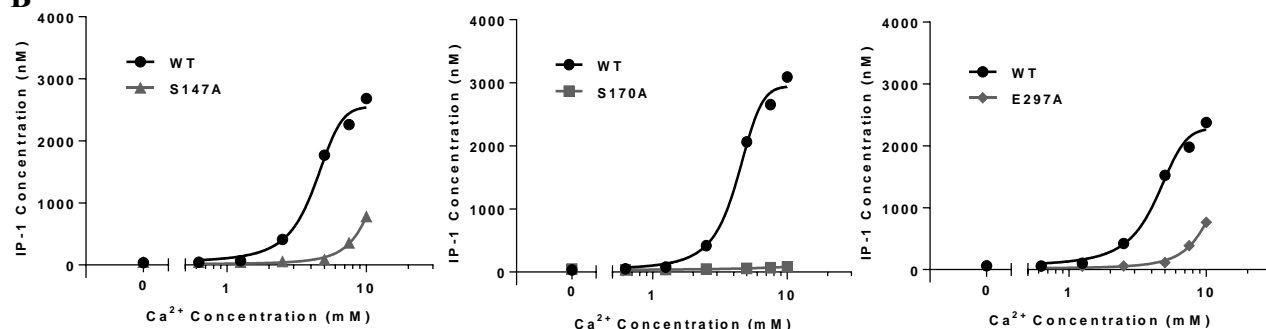
**Fig. S1 Detection of CaSR expression in HEK-CaSR whole cell protein by anti-CaSR antibody in western blot analysis.**

We confirmed anti-CaSR antibody specificity using whole protein fractions from CaSR-expressing HEK-293 cells (HEK-CaSR), HEK-293T cells (HEK), and HEK-293 cells transfected with full-length CaSR (WT). The amount of protein applied to each lane is as follows; HEK-CaSR: 1  $\mu$ g; HEK and WT: 10  $\mu$ g.

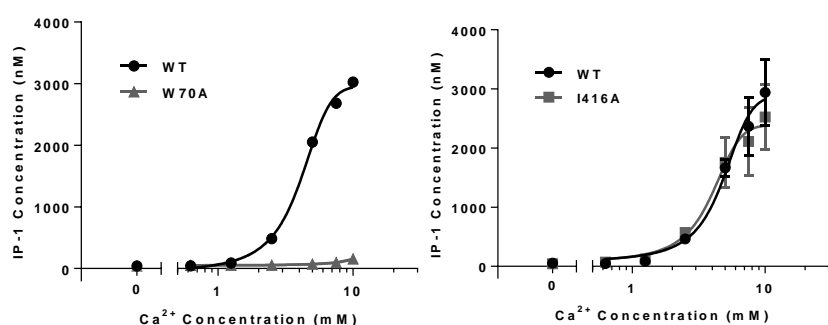
**A**



**B**



**C**



**D**

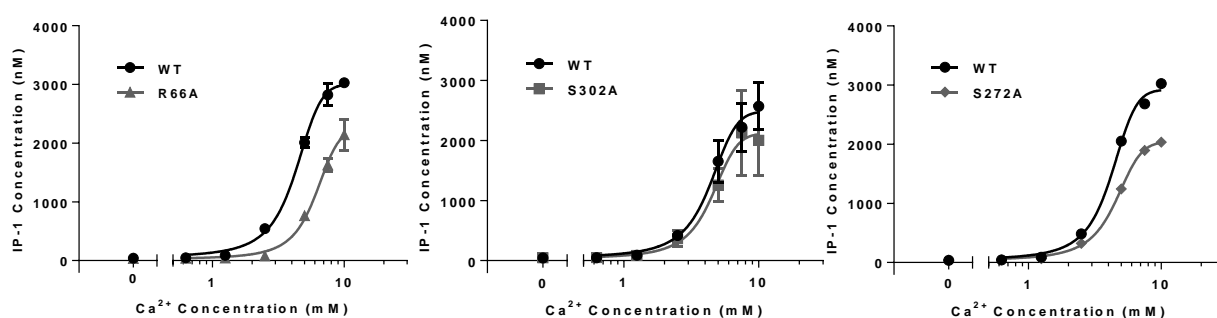


**Fig. S2 Effect of the mutation of CaSR protein on IP-1 accumulation of transiently CaSR expressing HEK-293T cells.**

Comparison of IP-1 accumulation between wild-type and mutant CaSR. (A) closed circle, WT; closed triangle, C482Y; closed square, E837A (B) closed circle, WT; closed triangle, S147A; closed square,



S170A; closed rhombus, E297A **(C)** closed circle, WT; closed triangle, W70A; closed square, I416A **(D)** closed circle, WT; closed triangle, R66A; closed square, S302A closed rhombus, S272A. Tests were performed in duplicate for each concentration. The number of tests was W70A, S170A, S272A, E297A, C482Y, E837A: n=1, S147A: n=2, and R66A, S302A, I416A: n=3, respectively. The Data are presented as mean values and  $\pm$ S.D. (presented when there are three independent results).

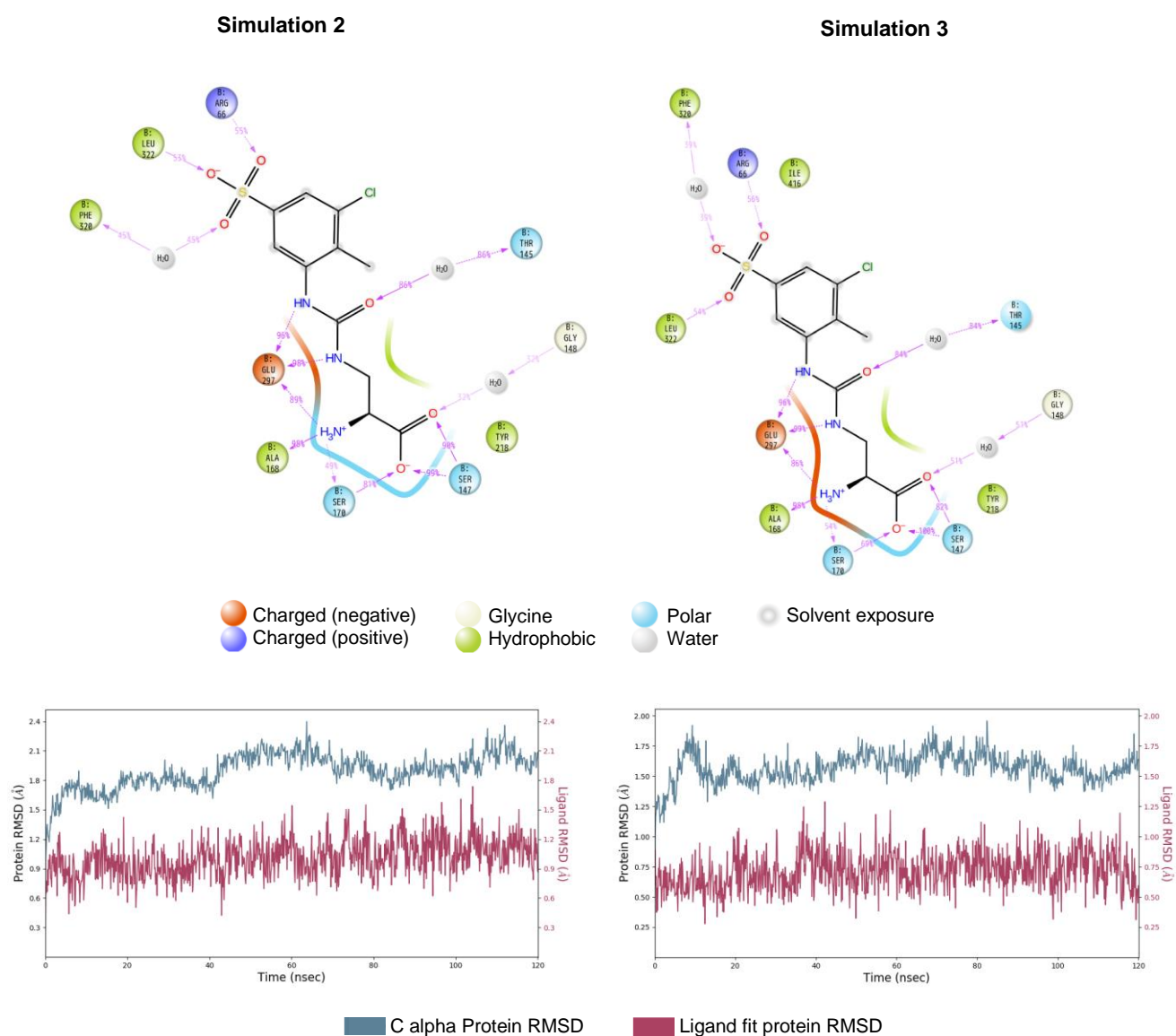


**Fig. S3 Estimation of upacalcet binding mode based on molecular dynamics simulation (simulation 2 and 3).**

2D summary of interaction analysis results of IFD rank 37 of PDB 5FBH chain B during 120 ns of molecular dynamics simulations. The interaction pairs that occur during more than 30% of the simulation time are included (top). The RMSD of protein and ligand relative to the starting complexes during 120 ns of molecular dynamics trajectory (bottom).